Schiff Base Complexes and their Assemblies on Surfaces

Minna Räisänen

Laboratory of Inorganic Chemistry
Department of Chemistry
Faculty of Science
University of Helsinki
Finland

Academic Dissertation

To be presented, with the permission of the Faculty of Science of the University of Helsinki, for public criticism in Auditorium A110 of the Department of Chemistry, A. I. Virtasen aukio 1, on June 13th 2007 at 12 o'clock noon.

Helsinki 2007

Supervisors

Professor Markku Leskelä
and
Professor Timo Repo
Laboratory of Inorganic Chemistry
Department of Chemistry
University of Helsinki
Finland

Reviewers

Professor Helge Lemmetyinen
Institute of Materials Chemistry
Tampere University of Technology
Finland

Professor Kari Rissanen
Laboratory of Organic Chemistry
Department of Chemistry
University of Jyväskylä
Finland

Opponent

Professor Kyösti Kontturi
Laboratory of Physical Chemistry and Electrochemistry
Department of Chemical Technology
Helsinki University of Technology
Finland

ISBN 978-952-92-2148-6 (paperback)
ISBN 978-952-10-3972-0 (PDF)
http://ethesis.helsinki.fi

Yliopistopaino
Helsinki 2007

Abstract

Schiff bases and their transition metal complexes are of significant current interest even though they have been prepared for decades. They have been used in various applications such as catalysis, corrosion protection, and molecular sensors. In this study, *N*-aryl Schiff base ketimine ligands as well as numerous new, differently substituted salen and salophen-type ligands and their cobalt(II), copper(II), iron(II), manganese(II), and nickel(II) complexes were synthesised. New solid state structures of the above compounds and the dioxygen coordination properties of cobalt(II) complexes and catalytic properties of three synthesised binuclear complexes were examined. The prepared complexes were applied in the formation of self-assembled layers on a polycrystalline gold surface and liquid-graphite interface. The effect of metal ion and ligand structure on the as-formed patterns was studied. When studying gold surfaces, a unique thiol-assisted dissolution of elemental gold was observed and a new thin gold foil preparation method was introduced.

In the summary, synthesis, structures, and properties of Schiff base ligands and their transition metal complexes are described in detail and the applications of these reviewed. Assemblies of other complexes on a liquid-graphite interface and on a gold surface are also presented, and the surface characterisation methods and surfaces employed are described.

Preface

This work has been carried out during the years 2003-2007 at the Laboratory of Inorganic Chemistry, University of Helsinki including several research visits to the Department of Materials and Catalysis, University of Ulm, Germany.

I am most indebted to my supervisors, Professors Markku Leskelä and Timo Repo, for providing the opportunity to accomplish my PhD studies under their professional guidance and for their support during these years.

I am most grateful to Professor Bernhard Rieger, University of Ulm, for our collaboration and for providing the opportunity to visit his group and to use the research facilities therein. I am grateful to all group members for their friendliness, especially Dieter Meinhard, Florian Mögele, and Marcus Wegner, and not least for all the arrangements related to my visits. I highly appreciate the contributions of Florian and Dr. Ulrich Ziener, Department of Organic Chemistry III, Macromolecular Chemistry, University of Ulm, as well as of Dr. Michael Bolte, Institut für Anorganische Chemie, Johann Wolfgang Goethe-Universität Frankfurt am Main, Germany, to our joint publications.

It would not have been possible to realise this work without the friendly help and advice of several people. I am most grateful to Professor Pekka Pyykkö for the numerous, kind discussions. He and Dr. Nino Runeberg are kindly thanked for their contributions to this work. I would like to express my gratitude also to Dr. Pedro de Almeida, Kristoffer Meinander, Dr. Jorma Matikainen, Ph.Lic. Robert Roozeman, Dr. Fabio Donadini, Ph.Lic. Jyrki Viidanoja, Docent Marc Baumann, Ph.Lic. Pentti Jyske, Markku Hyttinen and Matti Laanterä for their valuable contribution to the studies presented in this thesis.

All former and present members of the Laboratory of Inorganic Chemistry, especially those of Catlab, are thanked for creating a pleasant working environment. I am most indebted to Docents Martti Klinga and Ilpo Mutikainen and more recently to Dr. Martin Nieger for kindly teaching and sharing with me their expertise in the field of crystallography. I am grateful to Dr. Marianna Kemell, Dr. Heikki Korpi, Dr. Antti Niskanen, Santeri Feodorow, Pertti Elo and Dr. Titta Aaltonen for their contributions to this work. I want to thank especially Drs. Mika Kettunen and Kristian Lappalainen for being such wonderful, encouraging advisors in the lab and Ahlam Sibaouih for all those nice conversations we had while we worked in the same lab.

Most importantly my family, Pirkko, Jyrki, Juha, Riikka, Iita, Aaro, Anja, Meeri and Lahja, deserve my deepest thanks for their continuous love and support.

The financial support of the Magnus Ehrnrooth Foundation, Acta Chemica Scandinavica and the University of Helsinki is gratefully acknowledged.

Vantaa, May 2007 Minna Räisänen

List of original publications

This thesis is based on the following publications:

I Räisänen, M. T.; Elo, P.; Kettunen, M.; Klinga, M.; Leskelä, M.; Repo, T.: Practical method for 2-hydroxyphenylketimine synthesis. *Synth. Commun.*, in press.

II Korpi, H.; Räisänen, M. T.; Leskelä, M.; Repo, T.: Binuclear cobalt and manganese salen complexes: synthesis, characterisation, and coordination of dioxygen. Submitted to *Polyhedron*.

III Räisänen, M. T.; Klinga, M.; Leskelä, M.; Repo, T.: 3D structures of Cu(salen) and 2D structures of Cu(salophen) complexes. Submitted to *Eur. J. Inorg. Chem.*

IV Räisänen, M. T.; de Almeida, P.; Meinander, K.; Kemell, M.; Mutikainen, I.; Leskelä, M.; Repo, T.: Cobalt salen functionalised polycrystalline gold surfaces. Submitted to *Thin Solid Films*.

V Räisänen, M. T.; Kemell, M.; Leskelä, M.; Repo, T.: Oxidation of elemental gold in alcohol solutions. *Inorg. Chem.* **2007**, *46*, 3251–3256.

VI Räisänen, M. T.; Runeberg, N.; Klinga, M.; Nieger, M.; Bolte, M.; Pyykkö, P.; Leskelä, M.; Repo, T.: Coordination of pyridinethiols in gold(I) complexes. Submitted to *Inorg. Chem.*

VII Räisänen, M. T.; Mögele, F.; Feodorow, S.; Rieger, B.; Ziener, U.; Leskelä, M.; Repo, T.: Alkyl chain length defines 2D architecture of salophen complexes on liquid-graphite interface. *Eur. J. Inorg. Chem.*, in press.

The publications are referred to in the text by their roman numerals.

Abbreviations

AAS	Atomic Absorption Spectroscopy
AFM	Atomic Force Microscopy
AES	Auger Electron Spectroscopy
DMF	Dimethylformamide
DMSO	Dimethylsulfoxide
ESCA	Electron Spectroscopy for Chemical Analysis
FTIR	Fourier Transform Infrared
HOMO	Highest Occupied Molecular Orbital
HOPG	Highly Oriented Pyrolytic Graphite
ISE	Ion Selective Electrode
LEED	Low Energy Electron Diffraction
LEIS	Low Energy Ion Scattering
LUMO	Lowest Unoccupied Molecular Orbital
2-PS	2-pyridinethiol
4-PS	4-pyridinethiol
RHEED	Reflection High Energy Electron Diffraction
salen	*N*,*N*'-ethylene-bis(salicylideneimine)
salophen	*N*,*N*'-*o*-phenylene-bis(salicylideneimine)
SAM	Self-assembled Monolayer
SEM	Scanning Electron Microscopy
SERS	Surface Enhanced Raman Scattering
SIMS	Secondary Ion Mass Spectrometry
SPR	Surface Plasma Resonance
STM	Scanning Tunneling Microscopy
TCB	1,2,4-trichlorobenzene
TEMPO	2,2,6,6-tetramethylpiperidine *N*-oxyl
THF	Tetrahydrofuran
UHV	Ultra High Vacuum
UPS	Ultraviolet Photoelectron Spectroscopy
XPS	X-ray Photoelectron Spectroscopy
XRR	X-Ray Reflectivity

Table of contents

1 Introduction

Schiff bases, named after Hugo Schiff (1834-1915), and their transition metal complexes continue to be of interest even after over a hundred years of study.[1-4] Schiff bases have a chelating structure and are in demand because they are straightforward to prepare and are moderate electron donors with easily-tunable electronic and steric effects thus being versatile.[5,6] Schiff base metal complexes are still widely used in catalysis but increasingly with a slightly modified concept.[5,7-19] Complexes have been immobilised on solid supports, such as alumina, silica, or polystyrene,[20-24] or assembled inside a DNA duplex.[25] However, the number of studies where Schiff bases have been used for construction of various nanostructures is increasing, and these uses are the focus of this study.[26-63]

Currently, a challenging task in nanoscience (defined here as science concerning itself with objects whose smallest dimensions are between a few nanometres and 100 nanometres)[64] is to arrange and connect molecules in well-ordered defined patterns. The pattern formation should be controllable as orientation and relative positions of the molecules are often important for obtaining useful properties.[65-67] Functional materials are of great interest for a variety of applications, such as nanodevice and nanomachine platforms and photoconductor, electrochromic or nonlinear optical materials.[65,66,68-70] First versions[71,72] of artificial molecular devices[73,74] were introduced in the 1970s and 1980s and at that time it was realised that molecules are probably the most convenient building blocks for construction of nanoscale devices and machines.[75,76] In addition, it is important to note that research into nanoscience and technology can be carried out and progress only with the existence of relevant characterisation techniques and their continual improvement and development, as well as the invention of new techniques.[77-79]

Self-assembly is an efficient and commonly employed method for fabrication of functional materials.[66,80] It is a bottom-up approach in which stable, well-defined structures are built atom by atom or molecule by molecule via encoding of molecular building blocks.[66,70] However, it should be remembered that in order to construct a molecular device by employing this methodology, a support for the device and an interface connecting the device to its environment should be also constructed. Indeed, a future challenge is to connect a self-assembled structure with functional properties to a macroscopic environment.[81]

2 Scope of the study

Research in the Laboratory of Inorganic Chemistry has traditionally been divided into thin films and catalysts. One aim of this study was to establish research topics where these areas could be combined in a novel way. Synthesis of the applied metal complexes should preferably be straightforward to put more emphasis on actual applications than synthesis. To fulfil the above criteria, studies of cobalt(II) Schiff base applicability for molecular level dioxygen sensors on gold surfaces were selected as a starting point. As a by-product of these studies, a novel procedure for elemental gold dissolution and procedure for preparation of thin gold foils evolved. Another application of interest for metal Schiff base complexes was to study the self-assembled patterns they form on liquid-graphite interface. The synthesised ligands and complexes and their properties were studied with multiple techniques.

3 Schiff bases

Strictly speaking Schiff bases are compounds having a formula RR'C=NR'' where R is an aryl group, R' is a hydrogen atom and R'' is either an alkyl or aryl group. However, usually compounds where R'' is an alkyl or aryl group and R' is an alkyl or aromatic group are also counted as Schiff bases.[82] The Schiff base class is very versatile as compounds can have a variety of different substituents and they can be unbridged or *N*,*N*'-bridged. Most commonly Schiff bases have NO or N_2O_2-donor atoms but the oxygen atoms can be replaced by sulphur, nitrogen, or selenium atoms.[6] In this study, attention was paid to the most common Schiff bases, especially to salen and salophen complexes.[I-IV and VII]

3.1 Ligands

3.1.1 Synthesis

There are several reaction pathways to synthesise Schiff bases.[5,82-89] The most common is an acid catalysed condensation reaction of amine and aldehyde or ketone under

refluxing conditions. The first step in this reaction is an attack of nucleophilic nitrogen atom of amine on the carbonyl carbon, resulting in a normally unstable carbinolamine intermediate. The reaction can reverse to the starting materials, or when the hydroxyl group is eliminated and a C=N bond is formed an imine can be formed.[82,90] Many factors affect the condensation reaction, for example the pH of the solution as well as the steric and electronic effects of the carbonyl compound and amine. As amine is basic, it is mostly protonated in acidic conditions and thus cannot function as a nucleophile and the reaction cannot proceed. Furthermore, in very basic reaction conditions the reaction is hindered as sufficiently protons are not available to catalyse the elimination of the carbinolamine hydroxyl group.[91] In general, aldehydes react faster than ketones in Schiff base condensation reactions as the reaction centre of aldehyde is sterically less hindered than that of ketone. Furthermore, the extra carbon of ketone donates electron density and thus makes the ketone less electrophilic compared to aldehyde.[90]

Even though the condensation reaction can be retarded or totally hindered by steric effects of the carbonyl compound and amine, it is important to be able to also synthesise sterically hindered metal complexes. These complexes have a significant impact on catalyst design as the ligand substituents can have a prominent effect on the catalytic activity of the prepared metal complex.[92,93] Our experiments have shown that sterically hindered *o*-hydroxyphenylketimines and pyrazolone-based ketimines can be obtained only with poor yields, or not at all when prepared under normal refluxing conditions with an acid catalyst.[I] For this reason, a new preparation method[94] was sought, which resulted in imine preparation in an autoclave in methanol at 200°C. In order to find the reasons for the enhanced ketimine yields with the autoclave method, a series of ketimines was prepared (Figure 1).[I] Previously, imines have been prepared in an autoclave at 150-265°C from a primary amine and ketone or aldehyde but it has been reported that sterically hindered imines cannot be synthesised by this method due to slow reaction rates and autocondensation.[95-98] In addition, several imines have been prepared from ketone and ammonia under elevated pressures.[97-101]

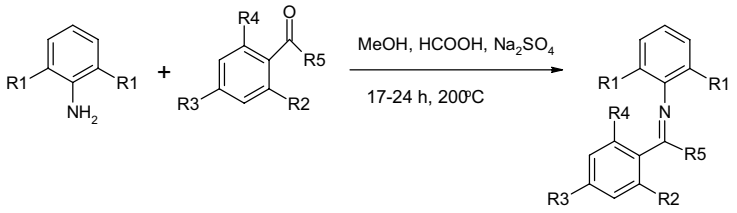

1; R^1 = Me, R^2 = OH, R^3 = H, R^4 = H, R^5 = Me
2; R^1 = Et, R^2 = OH, R^3 = H, R^4 = H, R^5 = Me
3; R^1 = *i*-Pro, R^2 = OH, R^3 = H, R^4 = H, R^5 = Me
4; R^1 = Me, R^2 = OH, R^3 = OH, R^4 = H, R^5 = Me
5; R^1 = Et, R^2 = OH, R^3 = OH, R^4 = H, R^5 = Me
6; R^1 = *i*-Pro, R^2 = OH, R^3 = OH, R^4 = H, R^5 = Me
7; R^1 = Me, R^2 = OH, R^3 = H, R^4 = OH, R^5 = Me
8; R^1 = Et, R^2 = OH, R^3 = H, R^4 = OH, R^5 = Me
12; R^1 = Me, R^2 = H, R^3 = OH, R^4 = H, R^5 = Me
13; R^1 = Et, R^2 = H, R^3 = OH, R^4 = H, R^5 = Me
14; R^1 = *i*-Pro, R^2 = H, R^3 = OH, R^4 = H, R^5 = Me
15; R^1 = *i*-Pro, R^2 = H, R^3 = H, R^4 = OH, R^5 = Ph

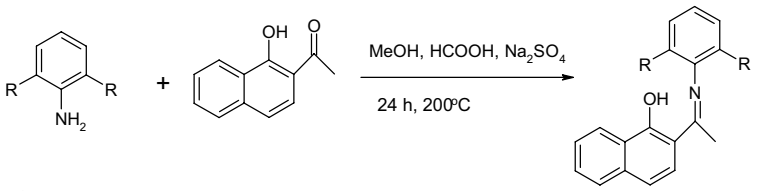

9; R = Me
10; R = Et
11; R = *i*-Pro

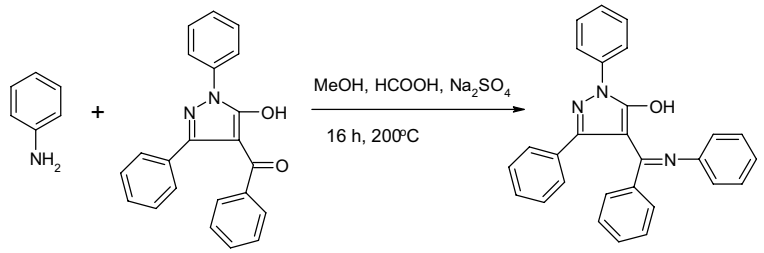

16

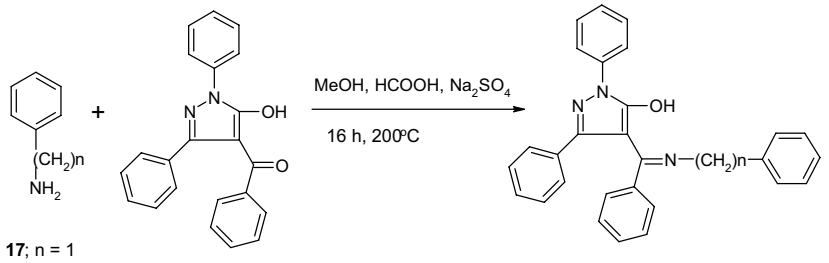

17; n = 1
18; n = 2

Figure 1. Hydroxyphenylketimines and pyrazolone-based ketimines prepared in autoclave at 200°C in methanol.[1]

The yields of *o*-hydroxyphenylketimines and their derivatives when prepared with the autoclave method were significantly higher compared with preparation under traditional refluxing conditions (Table 1). In contrast, the yields of *p*-hydroxyphenylketimines were virtually the same using both preparation methods (Table 1). Therefore it was concluded that the high temperature conditions help to overcome the energy barrier for *o*-hydroxyphenylketimine formation. The energy barrier is higher for *o*-hydroxyphenylketimines than *p*-hydroxyphenylketimines since the starting ketones for the former ketimines have an intramolecular hydrogen bond between the *o*-hydroxy group and the carbonyl oxygen.[102] The intramolecular hydrogen bond also exists in the *o*-hydroxyphenylketimines (Chapter 3.1.2).[I]

Table 1. Ketimine yields obtained with the autoclave method and the traditional condensation reaction under refluxing conditions. The yields have been recorded from ^{1}H NMR spectra.[I]

Ketimine	Yield[a] (%)	Yield[b] (%)	Ketimine	Yield[a] (%)	Yield[b] (%)
1	8	48	**10**	0	36
2	8	42	**11**	0	48[d]
3	[c]	46[d]	**12**	32	38
4	[c]	1[d]	**13**	22	23
5	7	28	**14**	28	32
6	4	21	**15**	0	6[d]
7	7	41	**16**	0	42[d]
8	2	12	**17**	0	36[d]
9	0	46	**18**	0	35[d]

[a]Conditions: 80°C, 24 h, HCOOH as catalyst, EtOH as solvent, Na_2SO_4 as drying agent.

[b]Conditions: 200°C, 24 h, HCOOH as catalyst, MeOH as solvent, Na_2SO_4 as drying agent. Reaction carried out in autoclave.

[c]Very low, not determined.

[d]Isolated yield.

Aldehydes used in the synthesis of *N,N*'-ethylene-bis(4-alkyloxysalicylidineimine) and *N,N*'-*o*-phenylene-bis(4-alkyloxysalicylidine-imine) (alkyloxy=OC_6H_{13}−$OC_{12}H_{25}$) were prepared according to a method in the literature.[103] Series of aforementioned salen and salophen ligand precursors together with other salen ligand precursors (the complexes

are presented in Figure 6 on page 20) were synthesised by the Schiff base condensation reaction at room temperature.[II,III,IV,VII] In the synthesis of salophen compounds, gummy-like crude products were obtained as powders after purification by stirring in methanol.[VII] Aldehyde 3-(*tert*-butyl)-5-formyl-4-hydroxyphenyl decanoate for the preparation of two ligand precursors (see Figure 6 on page 20 for complexes) was synthesised according to the method described by Jacobsen *et al.*[104] After synthesis, it was mixed with 2,5-di-*tert*-butyl-salicylaldehyde and ethylenediamine and they were stirred at room temperature under argon for 6 h. The two symmetrical and one unsymmetrical imines formed were separated by column chromatography.[104] A ligand precursor 1,1,3,3-tetra(salicylideneimino-methyl) propane for binuclear Co and Mn complexes was obtained via a three-step synthesis. First, 1,1,3,3-tetracarboxamidopropane was synthesised according to a method in the literature[105,106] and then reduced to 1,1,3,3-tetra(methylamine)propane. Finally, the prepared amine was condensed with salicylaldehyde and purified by recrystallisation.[II]

3.1.2 Structures, properties, and applications

In molecular crystals, short-range van der Waals interactions, repulsion forces, and hydrogen bonds (if appropriate donor and acceptor atoms are present in the molecule) determine the molecular packing. Hydrogen bonding affects the packing of molecules to a great extent and is the strongest interaction. Typically molecules are packed in such a way that a maximum number of hydrogen bonds are provided.[107]

Organic *N*-aryl Schiff bases prefer a non-planar conformation which can be explained by steric and electronic effects (Figure 2). Typically, the *N*-aryl substituent is twisted along the C−N axis by the angle $theta_1$ (see Figure 2), whereas the other aromatic ring is practically co-planar with the imine bond as the angle $theta_2$ is close to zero. The angle $theta_1$ increases when electron acceptor substituents are in the *para*-position of *N*-aryl amine or when alkyl and aryl substituents are in the imine bond, while it decreases due to donor substituents in the *para*-position of *N*-aryl amine. It should be noted that these are only approximate correlations and not always accurate. Substituting a hydroxy group in *ortho*-position of the Schiff base affects only slightly the overall conformation of the molecule.[6]

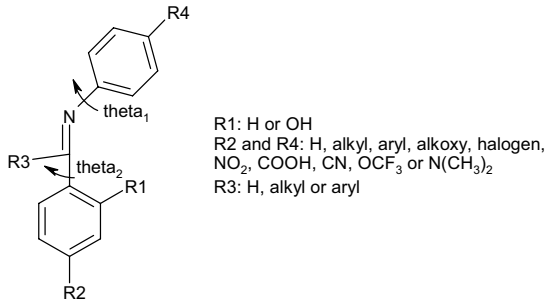

Figure 2. Schematic presentation of a non-planar conformation of N-aryl Schiff base.[6]

According to the crystal structures of ketimines **1**, **2**, **7**, and **8** (Figure 3), the angle $theta_2$ are 6.5(4)°, 5.7(3)°, 5.0(3)°, and 8.4(4)°, respectively. The angle $theta_1$ is 82.4(2)° for **1**, 83.9(2)° for **2**, 79.9(2)° for **7**, 85.9(2)° and for **8**. These ketimines have an intramolecular N1···O hydrogen bond where the donor atom in imines **1**, **2**, and **8** (enol forms) is oxygen, while in **7** (keto form) the donor atom is nitrogen. In the structure of **7** there is a second, intermolecular, hydrogen bond O1H···O2^{i} (i=-x+2, y+1/2, -z+3/2) with a distance 2.648(2) Å.[I] All observed hydrogen bond N1···O distances (2.544(2) Å in **1**, 2.545(2) Å in **2**, 2.456(2) Å in **7**, and 2.445(2) Å in **8**) are characteristic of hydrogen bonds as this distance is typically in the range of 2.490-2.574 Å.[108,I]

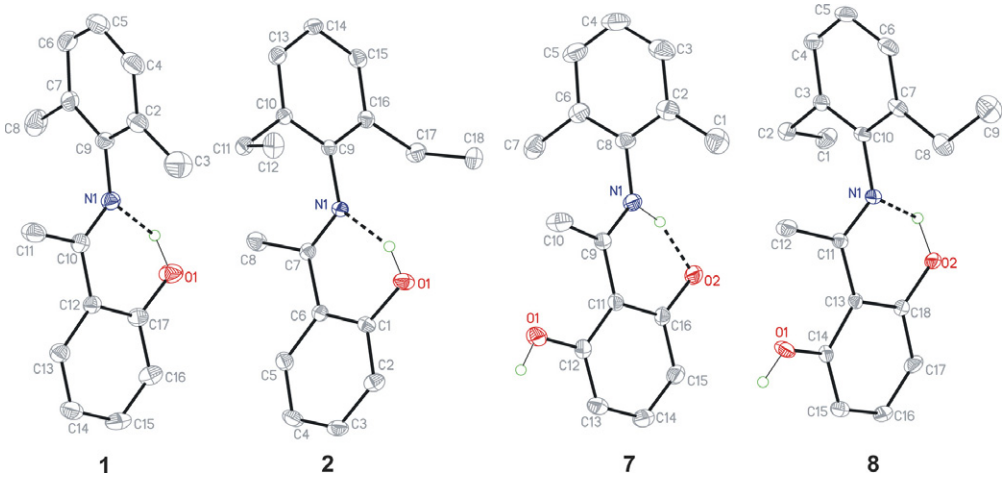

Figure 3. Molecular structures of o-hydroxyphenylketimines **1** and **2**, and 2,6-dihydroxyphenyl-ketimines **7** and **8** showing the intramolecular hydrogen bonds. Displacement ellipsoids appear at the 30% probability level. Hydrogen atoms, except those of the hydroxy and amine groups, have been omitted for sake of clarity.[I]

Imines whose syntheses were discussed above have different uses. *o*-Hydroxyketimines have served as starting materials for the preparation of aminophenols,[109,110] 4*H*-chromen-4-ylideneamines,[111] and 3,4-dihydro-2*H*-1,3-benzoxazines,[110,112] all of which possess interesting pharmacological properties. However, an attractive chemical use of the *o*-hydroxyphenylketimines, pyrazolone-based ketimines, and salen and salophen compounds prepared in this study is as a ligand precursor for transition metal complexes which can further be used in catalyst applications.[92-94,113] Substituents of Schiff bases affect their stability and reactivity and as an indication of this, Schiff bases are stabilised and made applicable for polymerisation reactions by introducing bulky groups into the phenoxy ring near the oxygen.[5] Specifically, salens have been claimed to be one of the most versatile ligands for metal complex catalyst generation.[25]

An interesting application of Schiff bases is their use as an effective corrosion inhibitor, which is based on their ability to spontaneously form a monolayer on the surface to be protected. For instance, compounds shown in Figure 4 have been studied in acidic or basic solutions aiming at corrosion protection of Al, Cu, and stainless steel.[26-43] Many commercial inhibitors include aldehydes or amines, but presumably due to the C=N bond the Schiff bases function more efficiently in many cases.[28] The principal interaction between the inhibitor and the metal surface is chemisorption.[29] The inhibitor molecule should have centres capable of forming bonds with the metal surface by electron transfer. In such cases the metal acts as an electrophile and the inhibitor acts as a Lewis base. Nucleophilic centres, such as oxygen and nitrogen atoms, of the protective compound have free electron pairs which are readily available for sharing. Together with the atoms of the benzene rings they create multiple absorption sites for the inhibitor thus enabling stable monolayer formation.[31,32] Recently, Schiff bases **A**-**D** presented in Figure 4 were studied as corrosion inhibitors for Al in hydrochloric acid solutions. They all proved to be excellent inhibitors but their activity was found to be strongly dependent on the substituents in the *N*-aryl moiety (**A** was the best inhibitor).[29]

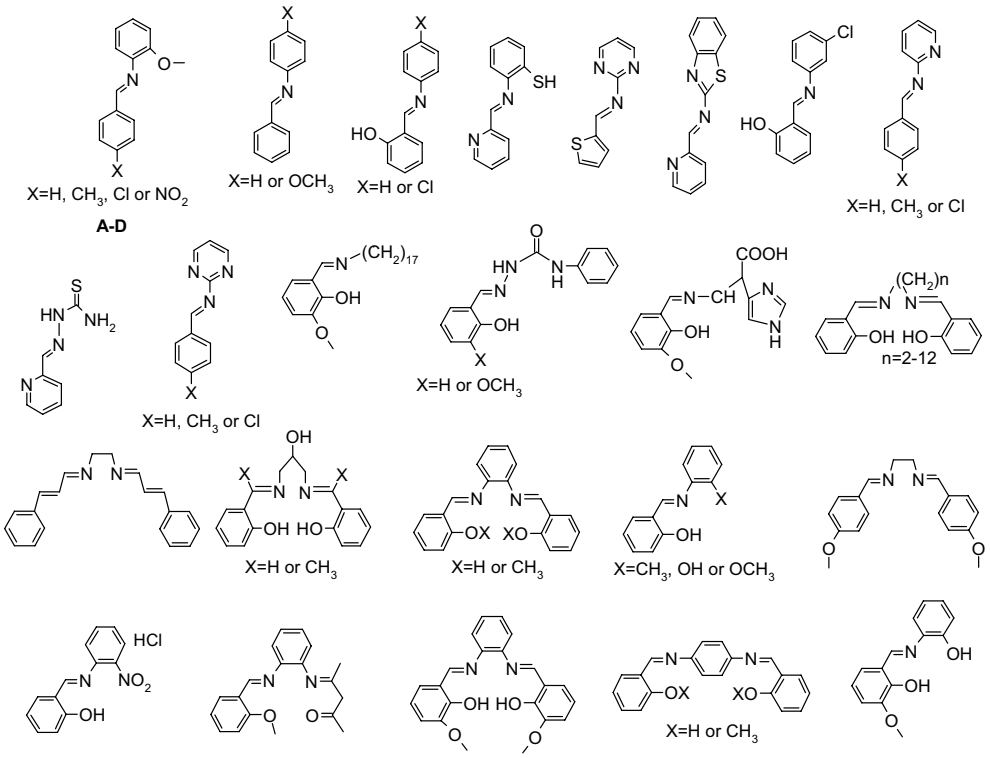

Figure 4. Examples of Schiff bases used as corrosion inhibitors for Al, Cu, and stainless steel in acid or basic solutions.[26-33,35,37-42]

A large number of different Schiff base ligands (Figure 5) have been used as cation carriers in potentiometric sensors as they have shown excellent selectivity, sensitivity, and stability for specific metal ions such as Ag(II),[44] Al(III),[45] Co(II),[46] Cu(II),[47-51] Gd(III),[52] Hg(II),[53] Ni(II),[54] Pb(II),[55] Y(III),[56] and Zn(II).[57] Indeed, from the ion sensor functional point of view it is crucial that the electroactive material dispersed in a polyvinylchloride (PVC) membrane exhibits strong affinity for a particular metal ion in order to enable selective permeation of one metal ion through the membrane electrodes.[47,50,55] Ion selective electrodes (ISEs) are widely used for monitoring metal ions in solutions since they allow accurate and fast analyses. In addition, they are easy to use, low-cost, can be used in a large number of samples, and generally do not require sample pretreatment.[54,57] Ion sensors are needed for example in environmental, agricultural, industrial, and medical analyses.[51]

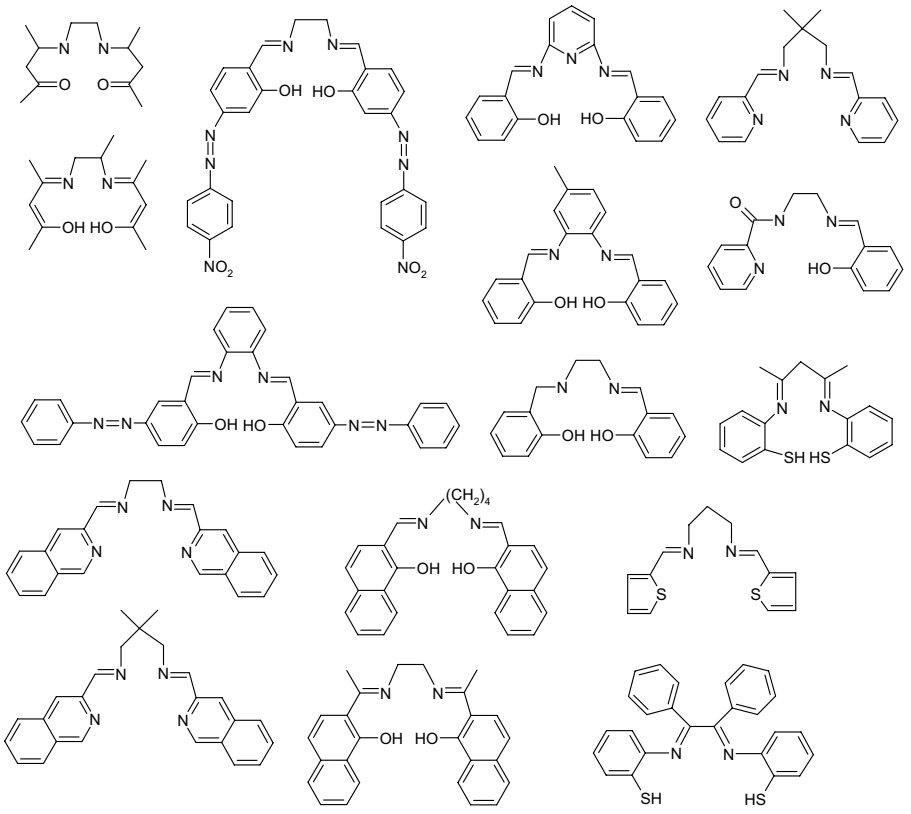

Figure 5. Schiff bases used as ionophores in ion selective electrodes.[45-57]

3.2 Complexes

3.2.1 Synthesis

Schiff base ligands can form adducts or chelates with metals depending on the reaction conditions used.[6] Review articles dealing with complexation of Schiff base ligands with metals have been published[5] and the synthesis of Schiff base adducts has been reviewed by Garnovskii *et al.*[6] and is not considered in this study. There are basically five different synthetic pathways for the preparation of salen and salophen-type metal complexes (the methods should be applicable to synthesis of other Schiff base metal complexes) and the method preferred depends on the metal. In four of the methods, the starting material is metal alkoxide, metal amide, metal alkyl or aryl compound, or metal

acetate or halide. In one of the methods, a sodium or potassium salt of the ligand is prepared first which is then reacted with metal halide. The ligand precursor could also be deprotonated by lithium bases but it is advisable to form sodium or potassium salt of the ligand.[5] Metal acetates are considered the most convenient starting materials for complexation with Schiff bases because they are soluble in alcohols and are salts of a weak acid.[6]

Co(II), Cu(II), Ni(II), and Mn(II) salen-type complexes of this study (Figures 6 and 7) were prepared by a direct reaction of the corresponding metal acetate and ligand precursor.[II-IV and VII] The solvents were selected so that the ligand precursors and metal acetates were fully dissolved but the complex precipitated out. All synthesised metal complexes were purified by washing with appropriate solvent and when necessary by recrystallisation. Ni and Cu complexes **22**-**27**, **32**-**39**, and **46**-**47** (Figure 6) were synthesised in air at room temperature. Cu complex **44** was prepared similarly to other Cu complexes but due to its high solubility it was very difficult to isolate. Even when a considerable amount of *n*-pentane or methanol was added to the reaction mixture, the complex did not precipitate. Finally, the powdered complex was obtained with a few percentage yield by slowly evaporating the solvents.[II-IV and VII]

All Co(II) and Fe(II) complexes were synthesised under argon using standard Schlenk techniques. Synthesis of Co(salen) complexes **19**-**21** (Figure 6) was carried out in several different ways with minor but significant modifications. The complex without coordinated dioxygen was obtained by adding the salen ligand precursor in dichloromethane into a methanol solution of Co acetate. After stirring at room temperature *ca.* for 20 h, the precipitate formed was filtered and the complex was obtained as an orange powder. When the solvent was changed from dichloromethane to chloroform, the complex did not form any precipitate. These Co(salen) complexes coordinate dioxygen very easily and it was observed that when the complex did not precipitate from the solution by itself, it was obtained with a coordinated dioxygen in the form of a dark brown solid. Therefore, the brown product was obtained when the complex precipitated from the solution only after removal of some solvent in a vacuum, or when methanol was added into the solution to obtain a precipitate of the complex. However, Co(salophen) complexes **28**-**31** (Figure 6), were not sensitive to the synthesis route used as they do not coordinate dioxygen so easily as corresponding salen complexes.[IV and VII]

For the preparation of Fe(II) complexes **40**-**43** (Figure 6), a sodium salt of the ligand was prepared first by adding NaH to a THF solution of the ligand precursor after which the complex was formed by adding $FeCl_2$. Both steps were carried out at room temperature.[114]

In addition to the aforementioned metal complexes, synthesis of Zn(salen) complexes with long alkyl sidechains was attempted from the ligand precursors and Zn acetate. However, the products were highly insoluble in common solvents. It has been reported that isolation of Zn(salen) is facilitated by the use of pyridine and without pyridine the complex can be isolated in a polymeric form where the oxygen atom of the Schiff base coordinates the zinc of another salen molecule.[5]

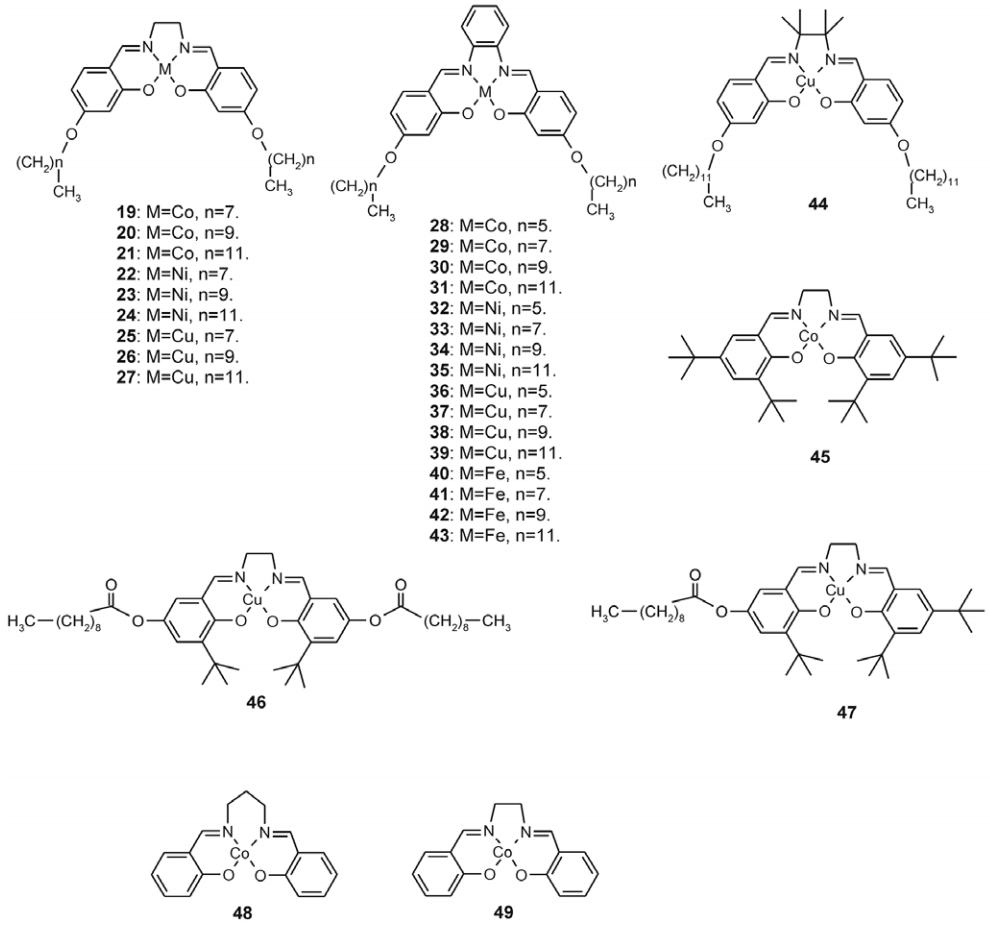

Figure 6. Synthesised metal salen and salophen complexes **19**-**49**.[II-IV and VII]

Homobinuclear complexes (**50**-**52**, Figure 7) were synthesised under argon by using standard Schlenk techniques. In all cases with short reaction times a side-product of mononuclear metal complex was formed and therefore the reaction mixtures were heated at 70°C for 20 h to ensure complete complexation. The reaction mixture was filtered while hot in order to separate soluble impurities (unreacted ligand, metal acetate, and mononuclear complex) from the binuclear complex. Finally, the product was washed with ethanol.[II]

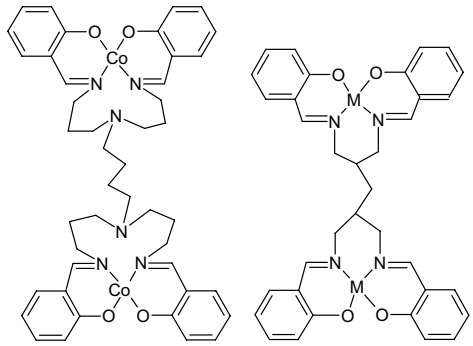

50 **51**: M=Co
52: M=Mn

Figure 7. Synthesised homobinuclear complexes **50**-**52**.[II]

3.2.2 Structures

In the following, emphasis is put on tetradentate metal salen and salophen complexes since their structures were studied via determination of five new single crystal structures of Cu and Co(salen) complexes. Co complex **45** crystallised easily in air from a mixture of toluene and acetone without oxidation of Co(II) (Figure 9, page 24).[IV] Four Cu(salen) complexes **25**-**27** and **27·MeOH** bearing long alkyl chains (C_8-C_{12}) in salicylidene moieties were crystallised from chloroform or dichloromethane–methanol (Figure 10, page 24).[III] Surprisingly, only few solid state structures of bridged Schiff base complexes bearing long (C_4-C_{16}) alkyl chains in the salicylidene moieties have been previously determined.[115-119] In addition, structures for salophen-type metal complexes bearing long alkyl chains do not exist. Only the structure for Fe complex with ethoxy-groups in the salicylidene moiety has been determined.[120] It seems that single crystals of salophen complexes bearing long alkyl chains are more difficult to obtain than crystals of

salen complexes. Furthermore, our attempts to crystallise salophen complexes with long alkyl sidechains failed, as micelles or microcrystals, rather than real single crystals, were always obtained.

Metal salen and salophen complexes have a tendency for square-planar geometry as the bridge between the imine moieties forces the *cis*-configuration around the metal centre, although in some cases a slightly distorted geometry towards tetrahedral form exists.[6] When the metal complex has square-planar geometry, the metal ion is in the plane formed by the N_2O_2-donor atoms and the two axial positions are free for coordination of solvent or other molecules.[121-126]

Metal salen complexes can have an umbrella, stepped, or planar molecular conformation (Figure 8) due to folding of the six-numbered metallocycles and the metal centre may deviate from the plane defined by the N_2O_2-donor atoms.[5,6] The umbrella and stepped forms are the most common for salen complexes and the strictly planar conformation has been reported only for few complexes.[5] According to structural data,[127,128] the umbrella form has been found in dimeric pentacoordinated complexes and in complexes having axial sites occupied by solvent or ligand molecules, whereas **27**·**MeOH**^{III} and Cu(acetylacetonate ethylenediamine)[129] have taken the umbrella conformation with minor distortion. Dimeric $Cu(salen)_2$ and $Co(salen)_2$ as well as Fe(salen)Cl have adopted the stepped form.[130-132] Size and oxidation state of the metal centre, possible axial ligands, and substitution of the salen affect the degree of folding in the stepped conformation. For instance, Cr(V) salen is folded while the corresponding Cr(III) salen is nearly planar.[5] It is assumed that the energy difference between possible conformations is not very large and for example Co(II) salophen crystallises as planar and umbrella isomers within the same unit cell.[6]

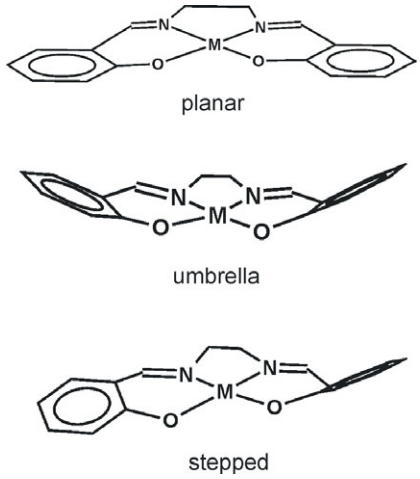

Figure 8. Schematic presentations of planar, umbrella, and stepped molecular conformations of salen complexes.[5]

Conformation of the ethylene-bridge is closely related to the overall conformation of the salen compound. Fully planar complexes might have an eclipsed conformation (N(1)–CH_2–CH_2–N(2) torsion angle *ca.* 0°) but usually the conformation is *gauche*. In *gauche*-conformation the carbon atoms of the ethylene-bridge are on the opposite sides of the MN_2O_2-plane. The geometry around the metal centre in *N*,*N'*-bridged Schiff base complexes may be tuned by altering the length of the bridge: the molecular structure becomes more flexible as the number of methylene groups in the bridge increases.[6] When the bridge consists of more than two methylene groups, the planar coordination around the Co ion changes closer towards a tetrahedral one.[133,134]

Single crystal structures of Co, Cu, and Ni(salen) and salophen complexes are considered below in more detail since these metal complexes were studied (II-IV and VII). Different ionic radii of Co, Cu, and Ni induce certain differences in the bond distances and angles of the metal salen and salophen complexes (Table 2).[121-126,135-147]

Table 2. Average bond distances (Å) and angles (°) calculated from the experimental crystallographic data[121-126,135-147] of M(II) salen and salophen complexes. In the case of Co, the values are for Co(I), Co(II) and Co(III). The ionic radii of four coordinated Ni(II), Co(II), and Cu(II) are 0.49, 0.56, and 0.57 Å, respectively. Ionic radius of six-coordinated Co(III) is 0.55 Å.[148]

	Ni(II)	Co(I/II/III)	Cu(II)
Bond			
M−O	1.85	1.90 / 1.86 / 1.89	1.89
M−N	1.86	1.82 / 1.85 / 1.89	1.93
Angle			
O−M−O	85.7	83.2 / 87.6 / 85.5	90.3
N−M−N	86.1	87.1 / 85.8 / 84.9	84.4
O−M−N	94.2	94.9 / 93.4 / 94.8	92.9
	175.5	176.5 / 177.1 / 178.0	172.8

In salen complexes **25**-**27**,[IV] and **45**[III] the geometry around the Cu(II) and Co(II) ion is a slightly distorted square-planar which is typical of salen complexes.[5,6] The basic coordination sphere of the Cu and Co ion consists of N_2O_2-donor atoms, whereas in **27·MeOH** an additional axially coordinated methanol solvent molecule results in an umbrella conformation. In all five structures the ethylene-bridge is in *gauche*-conformation.[III,IV]

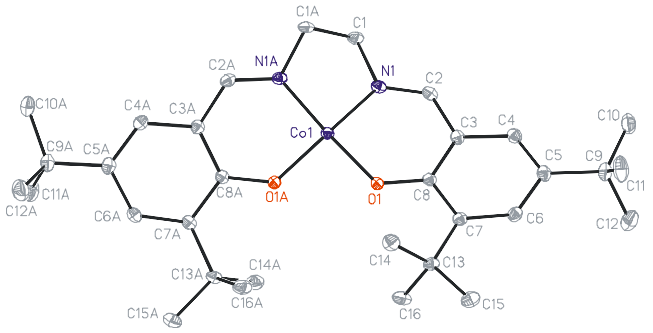

Figure 9. Molecular structure of Co complex **45**. The displacement ellipsoids are drawn at the 30% probability level and the hydrogen atoms have been omitted for sake of clarity.[IV]

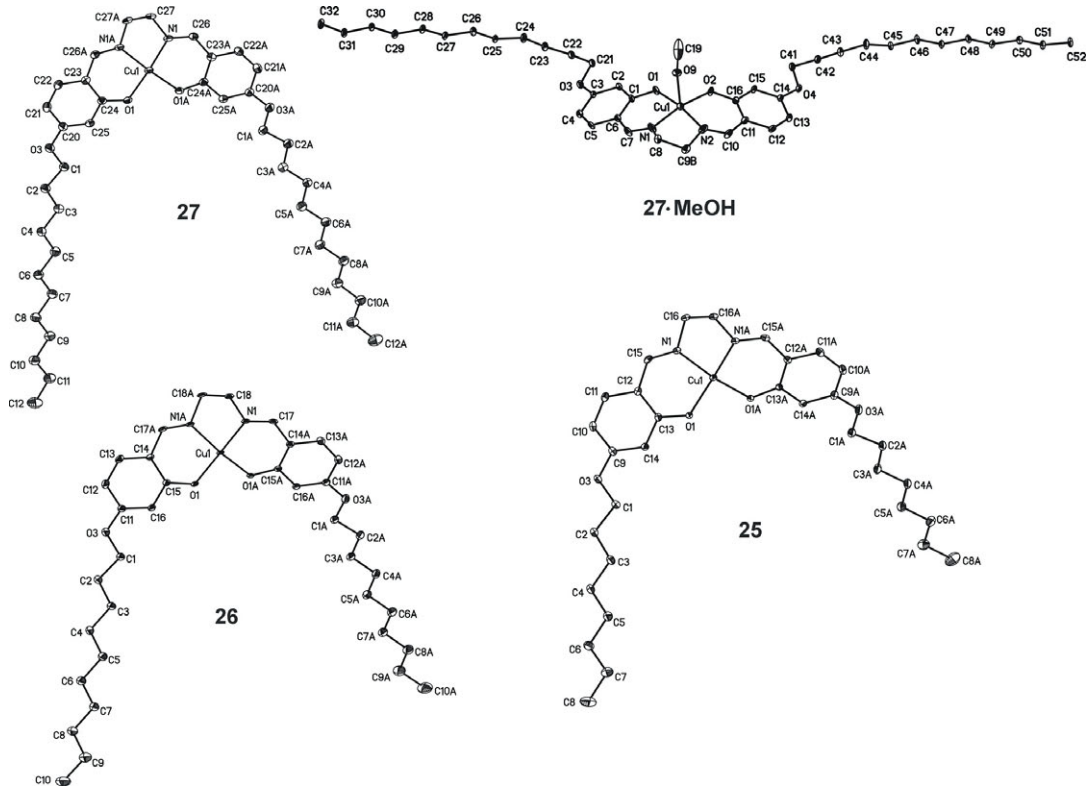

Figure 10. Molecular structures of Cu complexes **25-27** and **27·MeOH**. Displacement ellipsoids appear at the 30% probability level. Hydrogen atoms have been omitted for clarity. There is disorder in the ethylene bridge of **27·MeOH** and the carbon atoms had to be divided into two positions. However, the disorder is not shown for the sake of clarity. The distance between the Cu ion and the axial oxygen is 2.315(3) Å in **27·MeOH**.[III]

The MeOH molecule in the axial position of complex **27·MeOH** does not affect the bond lengths around the Cu ion as the Cu–O, Cu–N, and C=N bond lengths in **25**-**27** and **27·MeOH** are within the typical range for Cu(salen) complexes (Table 2). Instead, coordinated methanol has a significant effect on the spatial orientation (Figure 10) and packing of the complex. The unit cell packings of complexes **25**-**27** with different alkyl chain lengths do not differ significantly from each other as they are packed so that an alternating layered structure, which is typical of complexes with long alkyl chains,[149] is visible: layers consisting of alkyl chains alternate with layers consisting of salen moieties (Chapter 6.2.3.5).[III]

Different structure-property relationships can be observed in metal complexes. For example, in salen complexes absence or presence of an axially coordinating ligand can in general either reduce or enhance the folding of the metal complex, which further influences the transmission of chiral information. In theoretical studies, axial donor ligands have been shown to enhance enantioselectivity by shortening a metal–substrate distance in rate-determining stereoselective processes. In addition, conformation of the salen affects the approach path of the incoming substrate and the approach is not hindered even by bulky groups on the aromatic moiety. However, the orientation of the incoming substrate is controlled by the substituents. When a metal ion is complexed with a bi- or tridentate Schiff base, a dimeric metal complex can result. Especially early transition metals have the tendency to form stable, saturated complexes with octahedral geometry. These saturated complexes are catalytically inert but their formation can be prevented and the catalytic performance of the complex improved by introducing bulky substituents near the coordination sites.[5]

3.2.3 Properties

3.2.3.1 Dioxygen coordination

Synthetic dioxygen carriers are extensively studied and for example tertiary phosphine, salen, porphyrin, and phthalocyanine complexes of Co, Mn, Fe, and Cu have been found to coordinate dioxygen reversibly.[150,151] The activation of molecular oxygen with salen-type complexes was observed in the 1930s by Tsumaki[152] and since then has been under active research.[7,8,153-158]

Dioxygen coordination is an electron-seeking oxidative attack and its reversibility and rate depend significantly on the steric and electronic properties of the ligand substituents.[153,154] For example, in bridged Schiff bases an ethylene-bridge between the imine moieties results in complexes that coordinate dioxygen more easily than complexes with a phenylene-bridge or a tetramethylated ethylene-bridge.[154] In addition, the more planar the geometry of the complex is, the higher is its affinity for dioxygen.[159] The electron density donating substituents, such as alkoxy and halides, increase the coordination rate whereas substituents withdrawing electron density, such as alkyl and nitro groups, decrease it because they induce a lower charge density of the central ion

which in turn results in more difficult oxidation of the ion.[IV,155,156] However, Co salen-type complexes with *tert*-butyl groups in the salicylidene moieties have been reported to have a good affinity for dioxygen when the cyclohexyl-bridge between the imine moieties is functionalised with OH-groups hydrogen bonded to the coordinated dioxygen.[7]

The dioxygen coordination can occur via different modes, the preferred mode in each particular case depends on the ligand, and the species present in the solution if the complex is studied in solution.[160] For example Co(salen) and salophen complexes can form monomeric (superoxo) or dimeric (μ–peroxo) adducts with dioxygen in neutral solution or in a solid form.[7,21,153-155,161-163] The presence of a suitable donor solvent, such as DMF or DMSO, or of a monodentate base, all of which act as an axial ligand, facilitates the dioxygen coordination.[21,154,155] The base can be an aliphatic or aromatic amine, but pyridine and substituted pyridines are mostly used.[154] The axial base provides an additional stabilisation of the Co−O_2 bond through increase in electron density.[154,164]

In the salen and salophen complexes, which prefer square-planar geometry (Chapter 3.2.2), dioxygen is coordinated in one axial position and the other axial position is occupied by a base or solvent molecule.[126,154] The coordinated dioxygen is easily removed from the complex by heating, both in solution and solid state, in a stream of inert gas.[152,155,IV] Though numerous Co(salen) complexes activate dioxygen reversibly, there are still complexes, for instance (bis(salicylaldehyde)methylene-*p*,*p'*-diphenylenediaminato)-Co(II),[155] (di(salicylal)-3,3'-diimino-di-*n*-propylamine)-Co(II)[156] and *rac*- and *meso*-butane-2,3-diylbis(salicylideneiminato)Co(II), that have an irreversible dioxygen coordination.[157] In addition, for example di(*o*-hydroxyacetophenone)-ethylenediimine Co(II) has not shown any affinity for dioxygen.[156]

Dioxygen coordination properties of synthesised Co(salen) complexes **21** and **45**, and binuclear complexes **50-52** were studied by UV-Vis spectroscopy and the observed properties were compared with that of traditional unsubstituted Co(salen), **49** (Figures 11 and 12). Complexes **21**, **45**, **49**, and binuclear Co complex **50** coordinate dioxygen reversibly, but significant differences in their coordination rates were observed. Activity of **49** is considerably higher than that of **50**; it coordinates dioxygen within minutes when air is bubbled through the solution, whereas **50** must be in air contact overnight before similar changes can be seen in the spectrum. However, complex **51** showed an irreversible coordination, and the binuclear Mn complex **52** no coordination at all even when its solution was exposed to air for four days.[II,IV]

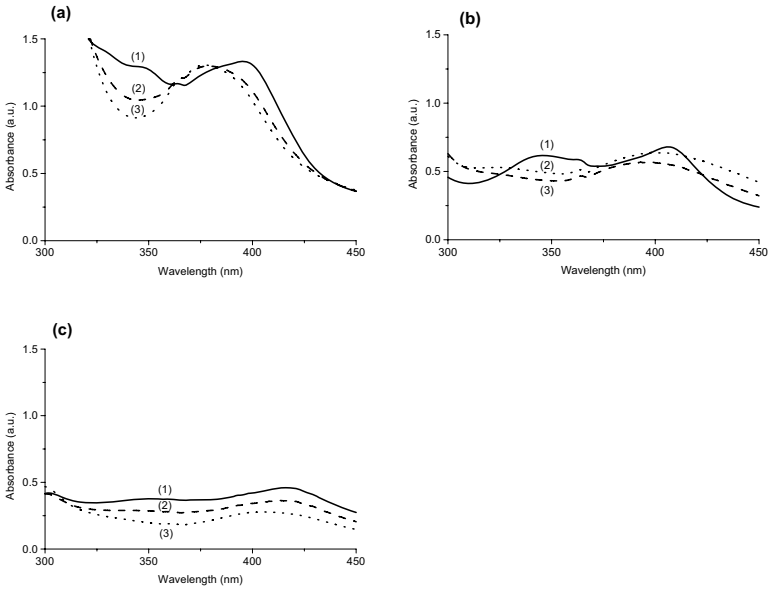

Figure 11. UV-Vis spectra of complexes a) **21**, b) **49** and c) **45** in DMF with pyridine as an axial base. Spectra (1) have been obtained under Ar atmosphere, spectra (2) after further storage in air for 30 min, and spectra (3) after 480 min storage in air.[IV]

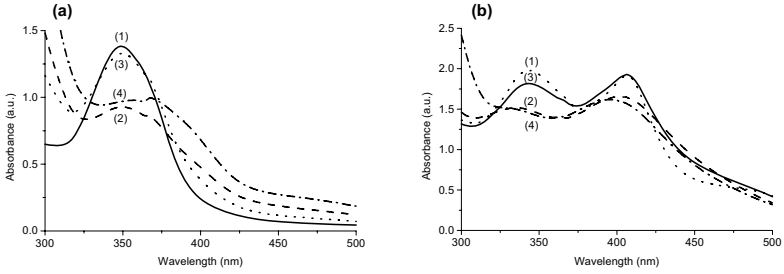

Figure 12. UV-Vis spectrum of DMF solution (pyridine as an axial base) of binuclear salen-type complex a) **51** and b) **50**. Spectrum (1) has been recorded from a cooled solution that has been heated at 100°C for 15 min with continuous Ar flow, spectrum (2) recorded after overnight exposure to air, spectrum (3) after second Ar treatment, and spectrum (4) after another overnight exposure to air.[II]

The different affinities of the Co complexes studied for dioxygen (**21**>**49**>**50**>**45**>**51**>**52**) can partly be explained by their electronic and geometric properties. Complexes **21** and **45** are fairly planar, but the former has electron density

donating alkoxy substituents, whereas the latter has electron density withdrawing *tert*-butyl substituents. In **50**-**52** the geometry around the metal ion is not as planar as in the other complexes studied and thus their ability to coordinate dioxygen is reduced. When more than two carbon atoms are added to the bridge between imino nitrogens, the planar conformation around Co ion changes towards tetrahedral.[II,IV]

3.2.3.2 Binuclear complexes and their catalytic activity in oxidation reactions

This chapter is dedicated to a short introduction of binuclear, more specifically homobinuclear, Schiff base complexes and to their use as catalysts in oxidation reactions. The existence of such a large number of binuclear complexes and reactions hinders a representative review here.

Complexes capable of reversible dioxygen coordination are commonly used as catalysts in oxidation reactions and Schiff base metal complexes have been studied for example in oxidation of phenols,[8,9,17] sulfides,[13,125] alcohols,[18] alkenes,[7] and lignin model compounds, such as 3,4-dimethoxybenzyl alcohol (veratryl alcohol).[19,II] In the catalytic redox chemistry with Schiff bases, it is important to control the deactivation of the system and possible dimerisation that can occur via coupling of the imino group. Imine bonds of the Schiff bases are quite vulnerable to reduction or nucleophilic attack and therefore reduction or alkylation must be considered as possible pathways for the deactivation of the catalyst when the Schiff base is used as a ligand.[5] The oxidation capability of the metal complex can be improved by changing the ligand substitution or by altering the ligand framework so that two metal centres are brought in a close proximity to form a binuclear complex.[165-169]

Even though binuclear complexes have been prepared for decades, they are still extensively studied because their physico-chemical properties and performances, such as magnetic properties and catalytic activities, can differ greatly from the analogous mononuclear species.[14,170-173] In many cases the activity of the binuclear complex is significantly greater compared with an equivalent mononuclear catalyst, but different reaction pathways and transformations specific to binuclear species have been reported.[174-177] In general, weak magnetic exchange coupling interactions between the metal centres are possible in binuclear complexes and the enhanced activities may be due to them.[173,178] The distance between the metal ions, the nature of the coordinating ligand and of the

bridging unit between the two metal centres, and the ligand orientation in ligand-bridged binuclear complexes, are crucial factors in creating and defining the character of the metal–metal interaction. The bridging unit should be able to mediate the interactions.[179-181] When two metal ions are coordinated at a suitable predetermined distance, they may have a tendency to coordinate and activate small molecules, such as dioxygen, between the metal centres.[174,178,182-186]

Catalytic activities of the synthesised binuclear Co and Mn(salen) complexes **50**-**52** (Figure 7, page 21) vs. analogous mononuclear complexes **48** and **49** were studied in the oxidation reaction of 3,4-dimethoxybenzyl alcohol by using dioxygen as an oxidant. The unsubstituted Co(salen) **49** gave a significantly greater aldehyde conversion (93%) than the binuclear complexes (0-13%) or **48** (7%), and it was concluded to be due to the bridge structure between the imino nitrogens. All complexes having more than two carbon atoms in the bridge had low activities, presumably due to the change from a planar geometry around the metal centre towards a tetrahedral one.[133,134,II]

4 Surface characterisation techniques used

Nowadays there is a wide variety of techniques available for surface characterisation and they can be classified under spectroscopic, microscopic, and other methods. The spectroscopic method is the most numerous and includes Fourier transform infrared (FTIR) spectroscopy, X-ray photoelectron spectroscopy (XPS), ultraviolet photoelectron spectroscopy (UPS), secondary ion mass spectrometry (SIMS), Auger electron spectroscopy (AES) and low energy ion scattering (LEIS). The microscopic includes atomic force microscopy (AFM) and scanning tunnelling microscopy (STM) and the other low energy electron diffraction (LEED), reflection high energy electron diffraction (RHEED), and X-ray reflectivity (XRR). All these can be considered as surface sensitive techniques.[187-190] Nonetheless, finally the properties of the surface to be characterised define the best method for each particular case. For instance, STM requires a conducting surface, AFM and STM smooth surfaces, and XPS, LEED and AES operate under UHV conditions. From the methods listed above, only FTIR and XPS (or electron spectroscopy for chemical analysis, ESCA, as it is also called), provide easily interpretable chemical data on the composition of surfaces. XPS is commonly used for SAM characterisation as it

provides information on the chemical bonding and oxidation state of all elements except hydrogen. The microscopic techniques allow structural imaging of SAMs but the chemical composition remains undetermined.[187-189]

Characterisation of SAMs requires sophisticated techniques as their thicknesses are up to a few nanometres. This means that the technique applied should be extremely surface sensitive, but equally important is the non-destructiveness of the technique. Three characterisation methods which were available for this study are described in more detail in Chapter 4.

4.1 X-Ray reflectivity

X-Ray reflectivity (XRR) is a surface-sensitive method for characterisation of thin-layer thickness, density, and surface and interface roughness. Samples can be made up of mono- or multilayers of different materials, but they must be less than 150 nm thick and rather smooth. In the measurement, a monochromatic X-ray beam is focused on the sample surface at a small angle of incidence. The scattering intensity of reflected X-rays is then recorded, and after normalisation plotted against the angle of incidence. By comparing critical angles and the number of interference fringes of the XRR curves, information on densities and thicknesses, respectively, of the samples can be obtained, whereas amplitude difference indicates total roughness (Figure 13).[190]

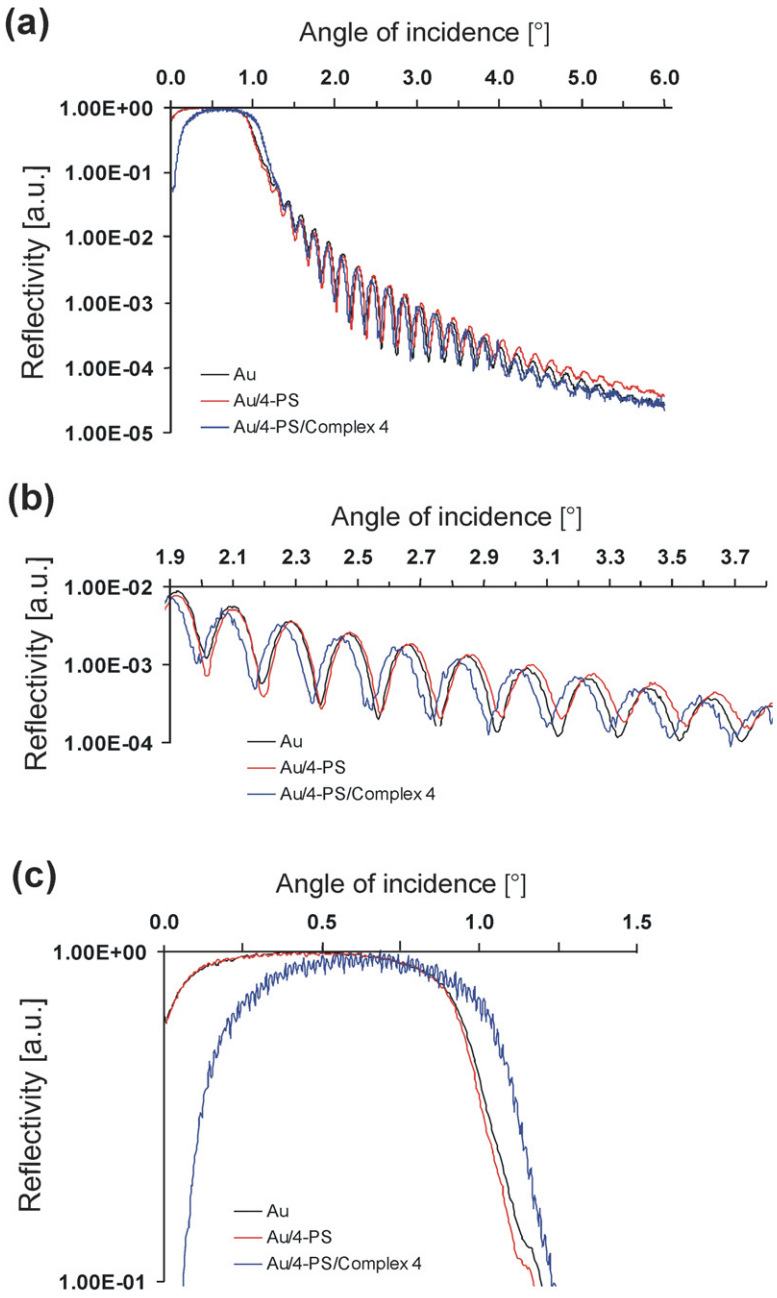

Figure 13. (a) X-Ray reflectivity curves for plain $Si/SiO_2/Au$ substrate, the substrate treated with 4-PS and the substrate treated with 4-PS and complex **21**. (b) Area of critical angles. (c) Area of amplitude differences. After 4-PS adsorption the total roughness of the substrate has increased and after the successive treatment with **21** the surface is smoother than in the previous stage. The surface treated with 4-PS and **21** is denser than the untreated and 4-PS treated surfaces.[IV]

4.2 Atomic force microscopy

Atomic force microscopy (AFM) was introduced by Binnig *et al.* in 1986.[191] It is a non-destructive technique that can be applied for construction of 3D topographic images of conducting, semiconducting, and insulating surfaces.[188] Besides surface imaging, AFM enables surface manipulation at an atomic level when a particularly stiff cantilever is used.[192,193] With this method and scanning tunnelling microscopy (STM), large surface areas in a range of 250 μm laterally and 15 μm vertically can be also studied, having importance for applications in surface sciences. Typically, during a measurement several atoms of the AFM tip interact with the surface. An atomic lateral resolution, compared with the typical resolution of *ca.* 1 nm, is achieved only with an unconventionally sharp tip and flat sample surface. The lateral resolution depends on the scan range since for scans up to 130 μm the resolution is a few nanometers but for smaller ranges it can be at the atomic scale. Because the photodiode used to track the position of the tip is very sensitive (*ca.* 0.01 nm), the depth resolution of AFM is at the sub-ångström level.[188]

AFM can operate in a constant-height or a constant-force mode, which are further divided into contact, non-contact, and tapping (also known as intermittent-contact) modes. In the contact mode, the tip touches the surface applying a continuous force on the sample, while in non-contact mode the tip vibrates near the surface. In the tapping mode, the vibrating tip taps across the surface.[192] During AFM measurement, a sharp ceramic or semiconductor tip mounted on a flexible cantilever scans over the surface. A piezoelectric transducer is used to scan the tip across the sample and a feedback loop ensures a constant separation between the tip and the sample. The force between the sample surface and the tip can be measured if it has a spring constant of about 0.1-1.0 N/m. This is more than an order of magnitude lower than typical spring constants between two atoms.[188]

The surface topography image is generated when the force between the sample and the tip is determined as a function of the position of the tip in three dimensions. When the tip approaches a distance of a few ångströms from the surface, repulsive van der Waals forces between the atoms of the tip and the surface cause the cantilever to deflect. The degree of the deflection depends on the tip-to-sample distance. To maintain a constant separation between the tip and the sample, the deflection of the cantilever from the reference line when the tip is repelled by or attracted by the surface must be measured accurately. The magnitude of the deflection is monitored most commonly by a laser diode that reflects at an oblique angle from the end of the cantilever into a position-sensitive

photodiode. A given cantilever deflection will then correspond to a specific position of the laser beam on the position-sensitive photodiode. Finally, when the laser deflection is plotted against the tip position on the surface, a topographic image of the surface is reproduced.[188,192]

A phenomenon known as tip imaging causes the main artefacts in AFM (and in STM). As long as the tip is much sharper than the feature imaged, the true edge profile is obtained. However, when the feature is sharper than the tip, the image will be dominated by the tip edges. Another type of artefact arises from the sensitivity of AFM to the rigidity of the sample surface. Soft surfaces can deform under the pressure of the AFM tip as in the contact mode there is a strong interaction between the tip and the surface.[188,192]

4.3 Scanning tunnelling microscopy

Scanning tunnelling microscopy (STM), invented in 1982,[194] is a non-destructive technique that can be operated under UHV conditions, in air and in liquid. Similarly to AFM, the best resolution is obtained under UHV.[187] The measurement principle is based on the quantum-mechanical tunnelling effect due to the wave nature of electrons, limiting the method for conductive samples. Electrons can penetrate through the potential barrier between the sample and the probe tip, introducing an electron tunnelling current. STM uses this effect to obtain a surface topography image by raster scanning over the sample while measuring the tunnelling current. Due to distance dependency of the tunnelling process, only very thin layers, typically monomolecular, can be probed. Individual atoms and atomic-scale surface structures can be measured with a scan size usually smaller than 1 μm×1 μm. STM can provide higher resolution than AFM as the typical lateral resolution is 0.1 nm and a depth resolution of 0.001 nm can be achieved.[187,188] Besides surface topography imaging, STM is used for surface lithography and manipulation.[193,195-199]

STM operates in a constant-current or a constant-height mode. In the former, the topography is defined by a constant tunnelling current at a given voltage bias, and in the latter the distance between the tip and the sample is kept constant. The use of constant-height mode enables faster measurement than the constant-current mode as the tip-to-sample distance stays constant, but it can be employed only for locally smooth surfaces. However, the constant-current mode can be used for rougher surfaces but the lateral

resolution is normally poorer because of the required feedback loop and the noise it induces in the data obtained.[192]

Tunnelling current (I_t) is induced between the metal tip and the conducting surface when the tip end, which in an ideal case consists of one atom, is brought to a distance of a few ångströms from the surface and a bias voltage (V_t, ≤1.5 V) is applied. I_t depends exponentially on the tip-to-sample distance (d), and linearly on the electronic local density of states at the Fermi level, evaluated at the location of the tip. Similarly to AFM, in its most common operation mode STM employs a piezoelectric transducer to scan the tip across the sample. Because of the precision of the piezoelectric scanning elements and the exponential dependence of I_t upon d, STM can provide images of individual atoms assuming that a single atom of the tip is imaging a single atom on the sample surface.[188,192]

Mechanical and electronic structure of the tip has considerable influence on the quality of an STM image. Tungsten tips, which are sharpened by electrochemical etching, can be used for a few hours in air until they oxidise. Alternatively, Pt-Ir tips can be prepared by cutting a wire with wire cutters. The latter tips are easy to make and they oxidise slowly, but their aspect ratio is not as high as that of tungsten tips and therefore tungsten tips are normally used for imaging large structures.[187,188]

Besides the tip imaging mentioned in Chapter 4.2, artefacts can arise from the sensitivity of STM to local electronic structure. Regions of variable conductivity will be convolved with topographic features; for instance an area of lower conductivity will show as a pit in the image. Distinguishing topographic and electronic effects can be difficult if the surface studied is not well known. An obvious drawback of STM is its requirement for conducting surfaces.[188]

5 Surfaces functionalised with self-assembled monolayers

5.1 Self-assembled monolayers

Self-assembly can be defined as “a spontaneous association of molecules under equilibrium conditions into stable, structurally well-defined aggregates joined by non-covalent bonds”.[200] Self-assembled monolayers (SAMs) on substrate surfaces were first

demonstrated by Zisman *et al.* in 1946 with various compounds on platinum.[201] The SAM methodology is a bottom-up approach which is widely used because large surface areas with well-defined composition, structure, and thickness can be easily formed.[80,202-24] In addition, head and anchoring groups of the adsorbate molecule can be varied to control the properties of the SAM formed and in fact for many applications an amphifunctional adsorbate is required.[202,205]

The thickness and composition of a SAM are defined by the SAM forming compound, assuming that the compound does not decompose. However, the structure formed can be dependent on the solvent used.[80,206] The self-assembly on the surface can occur from liquid or gas phase,[207,208] but here only the liquid phase is considered as the SAMs of this study were prepared from solutions.[IV,V,VII] The formation of monolayers at the liquid-solid interface can also be induced under electric potential. The electrochemical method utilises an electric potential to increase the affinity of the adsorbate for conductive substrates.[209] In addition, molecule assemblies can be stabilised by co-adsorption with other compounds.[210,211]

Self-organisation into ordered and highly packed 2D polycrystalline films requires that the molecules upon deposition on a substrate surface are mobile to allow them to form the most stable assembly.[62,205,212-214] The SAMs must be kinetically and thermodynamically stable in the long-term in order to maintain the desired applicational function. Adsorbate−adsorbate interactions, for example hydrogen bonds and van der Waals interactions, within the 2D arrays and adsorbate−substrate interactions exhibit strong driving forces for the formation of highly-ordered surface structures.[206,210,211,215-218] Besides providing stabilisation and mutual recognition of the SAMs, long alkyl chains act as easily variable spacers.[60,211] The adsorbate−substrate interactions of metal complex SAMs are due to the electrostatic interactions between the metal ion and the substrate, as well as to the alkane chain−substrate interaction.[211]

The focus of SAMs is nowadays on possible functional applications and therefore this methodology is used for constructing nanostructures.[80,213,215,219-221] It has been stated that SAM formation is the first step in all assembly and interface engineering.[222] The SAMs most often studied on transition metal surfaces all have a thiol-functionality but there are other functionalities that react with the substrate surfaces. Reactive functional group/surface –pairs are for example SH/Au,[212,215] S−S/Au,[215] COOH/Au,[223,224] SH/Ag,[215] COOH/Ag,[215] SH/Cu,[215] SH/Pt,[215] OH/Si[225] and OH/SiO_2.[225]

5.2 Surfaces

In the studies included in this thesis, the substrates used consisted of transition metal[IV,V] and graphite surfaces.[III,VII] Therefore, only these are discussed in this chapter, even though for instance hydroxylated silica substrates[215,226] have been studied extensively.

5.2.1 Gold

Metal surfaces can be either polycrystalline or single crystalline, the latter being smoother. The commonly used transition metal substrates for construction of SAMs are Cu, Ag, Au, Pt, and Pd but Au is used most often. When compared to Cu and Ag, Au is chemically more stable as it does not oxidise under ambient conditions and therefore its handling is easier.[227] In this chapter focus is put on thiol SAMs on Au, which have been prepared both under inert gas and in air, as these constitute the systems studied.[IV,V] High affinity of gold to sulphur can be explained by the Hard–Soft Acid Base (HSAB) principle. According to this principle soft acids, such as metal surfaces, prefer to react with soft bases (e.g. RSH and RS^-) rather than with hard bases (e.g. RNH_2, ROH, and RO^-).[228,229]

Analogous alkanethiols and alkyl disulfides adsorb on Au surfaces as gold thiolate (Au^+RS^-) species via the cleavage of S–H or S–S bonds, respectively, and the successive formation of a strong S–Au bond (*ca.* 40 kcal mol^{-1}).[204,206,215,216,230-236] The bonding proceeds basically in two phases. First, the thiol is adsorbed on the surface in a matter of seconds and then, during the following hours, the molecules in the formed SAM are rearranged in a more ordered way. The adsorption kinetics of the first phase is suggested to be a mixture of inseparable physical and chemical processes governed by surface−headgroup interactions in contrast to the orientation/ordering step that is governed by intermolecular interactions.[80,216,218] Typically, with longer immersion times more ordered SAMs are achieved.[216] Aromatic thiol SAMs are less extensively studied and their formation is not so well understood than those of alkanethiols, but they are still highly interesting, for example for molecular electronics applications. Electrons in the benzene rings are more delocalised than in alkyl chains causing a better electrical conductivity through the aromatic thiols.[218,237]

Organothiols have been reported to produce vacancy islands, one (maximum three) gold atom deep, on gold surfaces (Figure 14). The thiol adsorption causes an enhanced mobility of the gold atoms in the topmost layer leading to surface reconstruction. The lateral mobility takes place via hole migration and coalescence and it might be an intermediate step in the formation of gold thiolate complexes.[235,236,238] The vacancy islands, i.e. etch pits, were first observed on surfaces treated with alkanethiols and later on surfaces treated with partially or fully aromatic thiols.[239] In a theoretical study, adsorption of methylthiolate on Au(111) surface was studied by calculations based on the density functional theory, and showed that adsorbate-induced reconstruction enhanced the adsorption of molecules at the defected surface.[230]

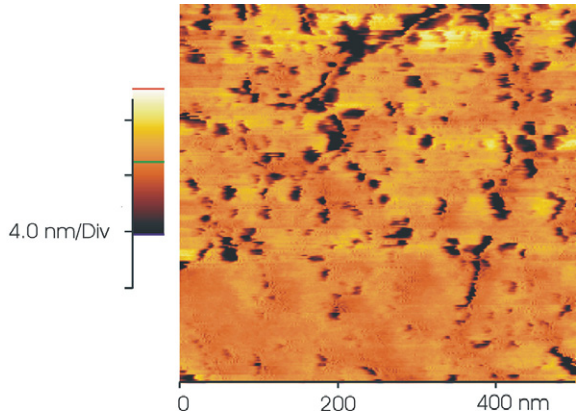

Figure 14. AFM-micrograph showing the etch pits formed in polycrystalline gold by 4-pyridinethiol adsorption (8 mM alcohol solution, 1 h).[IV]

The formation of vacancy islands, which are filled with an ordered thiol SAM, can be affected by the choice of the experimental conditions even though the thiol alkyl chain length has no effect on the etch pit depth and dioxygen has no significant effect on the pit formation in general.[236,238,240] By extending the immersion time of the gold substrate in the thiol solution, the surface coverage of monoatomic deep etch pits is increased. However, when the SAM formation is carried out at elevated temperatures, fewer depression pits result on the surface but the average size of the pits is considerably increased.[241,242] Moreover, it has been reported that thermal annealing revokes these defects.[238,243,244]

Besides producing vacancy islands on gold surfaces, thiol SAMs have been observed to result in protruding gold islands. It has been also suggested that the protruding

islands are caused by the increased mobility of surface gold atoms which then aggregate and form the islands. The mobility is due to the strong Au−S bond that loosens the gold atom adhesion within the two topmost layers.[218]

In the present study using AFM,[IV] it was noticed with polycrystalline gold surfaces prepared by vapour deposition that several factors affect the gold thin film surface structure and roughness. Glass as a substrate did not provide sufficiently smooth surfaces and therefore the gold thin films were prepared on Si(100) wafers. In addition, if a thin titanium layer was evaporated between the substrate (glass or silicon) and the gold film in order to obtain better adhesion, the resulting gold thin films were not the smoothest possible. The smoothest gold thin layer was obtained when the wafer was first oxidised thermally at 1000°C to form an approximately 150 nm thick SiO_2 layer. After evaporation of *ca.* 30 nm thick gold layer at room temperature, the wafer was annealed in air at 250°C for 3 h to increase the grain size, which resulted in locally smoother surfaces. Similarly, the $Si/SiO_2/Ti/Au$ structures were prepared at room temperature by first evaporating about 35 nm of Ti on the native SiO_2 layer of a Si(100) wafer after which about 100 nm thick gold layer was evaporated. These structures have a slightly rougher surface than the $Si/SiO_2/Au$ structures.[IV]

5.2.1.1 Dissolution of elemental gold

Elemental gold is chemically dissolved in aqua regia and halogen containing solutions, or in the presence of air or hydrogen peroxide, in thiocyanate and cyanide solutions.[227] In addition, recently solid gold has been dissolved in chloroform solution of cetyltrimethylammonium bromide when dioxygen was used as an oxidant.[245] During our studies,[V] a new method to oxidise and fully dissolve solid gold was discovered. The dissolution occurs selectively in methanol and ethanol solutions of 4-PS and 2-PS (Table 3). In this system, dioxygen has an essential role as an oxidant: Au thin films were dissolved only in the presence of air, not under argon. A dominating side-reaction was the decomposition of 4-PS and the formation of elemental sulphur[234] and previously unreported formation of 4,4'-dipyridyl sulfide. The dissolution of gold did not occur in water solution, at least not during the period of several months, possibly because of the low solubility of the Au complex in aqueous media. Gold was etched also in THF solution of 4-PS at ambient conditions, but this process was slow and was not studied in detail. The

role of possible existing impurities on the Au surfaces for gold dissolution was fully excluded experimentally.[V]

Table 3. Oxidation of Au thin films. Reaction conditions: film area ca. 1 cm^2, 8 mM solutions of 4-PS, 2-pyridinethiol (2-PS) and 4,4'-dipyridyl disulfide (4,4'-PSSP), ambient conditions.[V]

Entry	Solvent	Thiol	Atmosphere	Substrate	Immersion time	Effect on Au
1	EtOH	4-PS	air	$Si/SiO_2/Au$	1 h	etch pits
2	EtOH	4-PS	air	glass/Ti/Au	2 d	dissolution
3	MeOH	4-PS	air	$Si/SiO_2/Au$	2 d	dissolution
4	H_2O	4-PS	air	glass/Ti/Au	several weeks	etch pits
5	EtOH	4-PS	Ar	glass/Ti/Au	several months	etch pits
6	EtOH	4,4'-PSSP	air	$Si/SiO_2/Au$	several months	etch pits
7	EtOH	2-PS	air	glass/Ti/Au	41 days	etch pits

The oxidation kinetics of elemental Au in a solution of 4-PS was studied in detail by varying temperature, dioxygen pressure, and 4-PS concentration. The resulting Au concentrations in solutions (determined by atomic absorption spectroscopy, AAS) from samples treated in different conditions were recorded as a function of time (Figure 15). Dissolution rate of the reaction increases considerably as a function of 4-PS concentration, whereas O_2-pressure has no clear effect. Temperature influenced the dissolution rate, and reactions performed at 80°C showed that the Au(I) complex is thermally unstable and decomposes.[V]

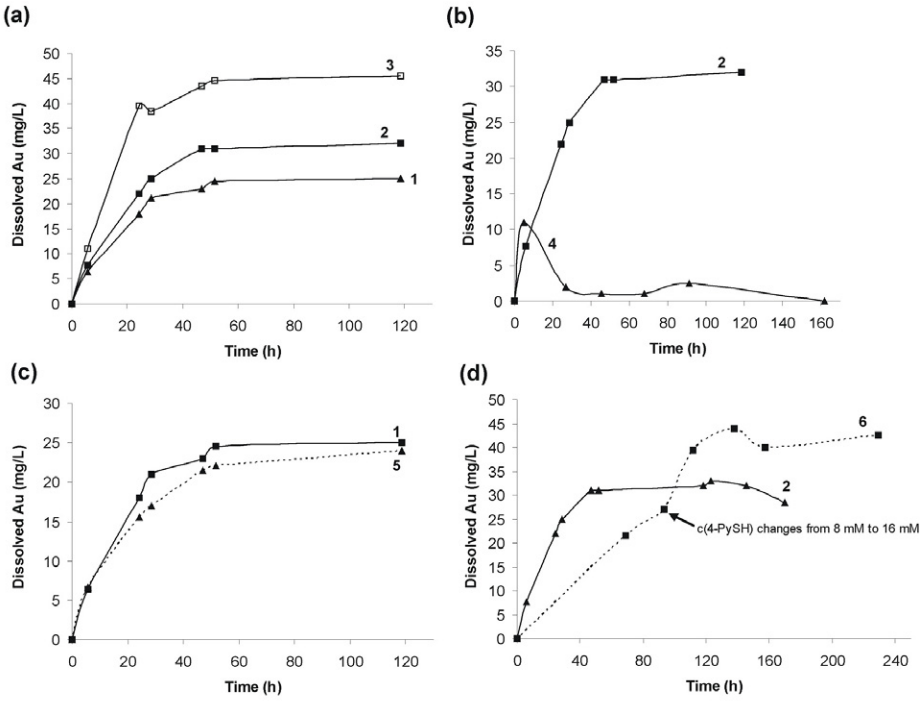

Figure 15. Effect of 4-PS concentration (a), temperature (b), O_2-pressure (c), and additional 4-PS (d) on the dissolution of Au nanoparticles. Experimental conditions: Au nanopowder (1 mg, particle size 30-130 nm), MeOH solution of 4-PS (15 ml). **1**: O_2-pressure 10 bar, c(4-PS)=8 mM, t 22°C. **2**: O_2-pressure 10 bar, c(4-PS)=16 mM, t 22°C. **3**: O_2-pressure 10 bar, c(4-PS)=40 mM, t 22°C. **4**: O_2-pressure 10 bar, c(4-PS)=16 mM, t 80°C. **5**: O_2-pressure 3 bar, c(4-PS)=8 mM, t 22°C. **6**: O_2-pressure 10 bar, the initial c(4-PS)=8 mM and after addition of extra 4-PS 16 mM, t 22°C.[V]

When gold thin films were treated in the presence of air in 8 mM EtOH solutions of thiophenol, pyridine or 4,4'-pyridyl disulfide (4,4'-PSSP), film dissolution did not occur within the monitored time periods. Since 4,4'-PSSP adsorbs on Au surface as thiolate and is inactive in the gold dissolution, it is suggested that the differing etching properties of 4-PS and 4,4'-PSSP are due to the zwitterionic form of 4-PS.[V] The thiol-thione tautomery distinguishes pyridinethiols also from thiophenol. The proposed reaction mechanism for gold oxidation is presented in Scheme 2. Based on the analysis used, it is suggested that the product is bis(pyridinium-4-thiolato)Au(I). Despite prominent efforts, the unambiguous structure of the labile counter ion remained unresolved. However, it is most probably to be methoxide or ethoxide depending on the solvent in which the reaction was carried out.[V]

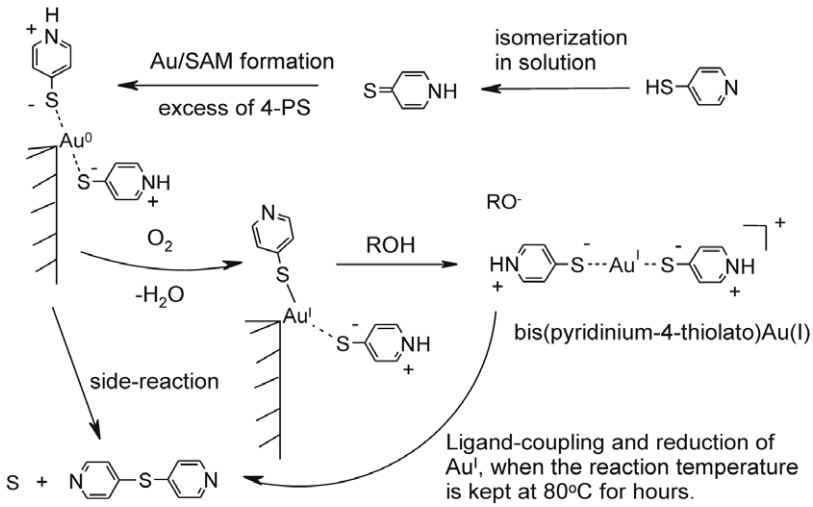

Scheme 2. Proposed oxidation reaction mechanism for Au^0 in methanol solution of excess of 4-PS.[V]

Tendency of pyridinethiols to coordinate with gold(I) in their zwitterionic form was noticed also during the synthesis of bis(pyridinium-2-thiolato)gold(I) chloride and bis(pyridinium-4-thiolato)gold(I) chloride. In these reactions, Au(III) is reduced to Au(I) when excess of 2- and 4-pyridinethiol is used and disulfide of the thiol is formed as a side-product.[VI]

5.2.1.2 Self-supporting thin gold foils

Traditionally gold thin films have been detached from substrates by pre-depositing a parting agent on the substrate prior to gold evaporation and finally dissolving the parting agent. The parting agent is a compound that does not react with gold, such as NaCl, KBr, KI, KCl, FeCl, plastic packing, or a sugar or soap solution.[246-250] Thin gold foils can be also prepared by pounding and in this case the foils are usually called gold leaves. Typical lower limit for foil thickness prepared by pounding is 100 nm.[251]

In this study, the dissolution of elemental gold was observed with 4-PS and later the dissolution ability of 2-PS was tested. Unexpectedly, by treating the gold film deposited on a Si/SiO_2 substrate in methanol or ethanol solution of 2-PS, the film was detached from the substrate and dissolved weeks later (Figure 16). Closer studies showed that thin films

(30 nm thick) are detached from the Si/SiO_2 substrate when treated in alcohol solution containing a mixture of 4-PS and 2,2,6,6-tetramethylpiperidine *N*-oxyl (TEMPO). The detaching was faster in the methanol solution of 4-PS/TEMPO than in the ethanol solution of 2-PS (*ca.* 14 h vs. 43 h).[V]

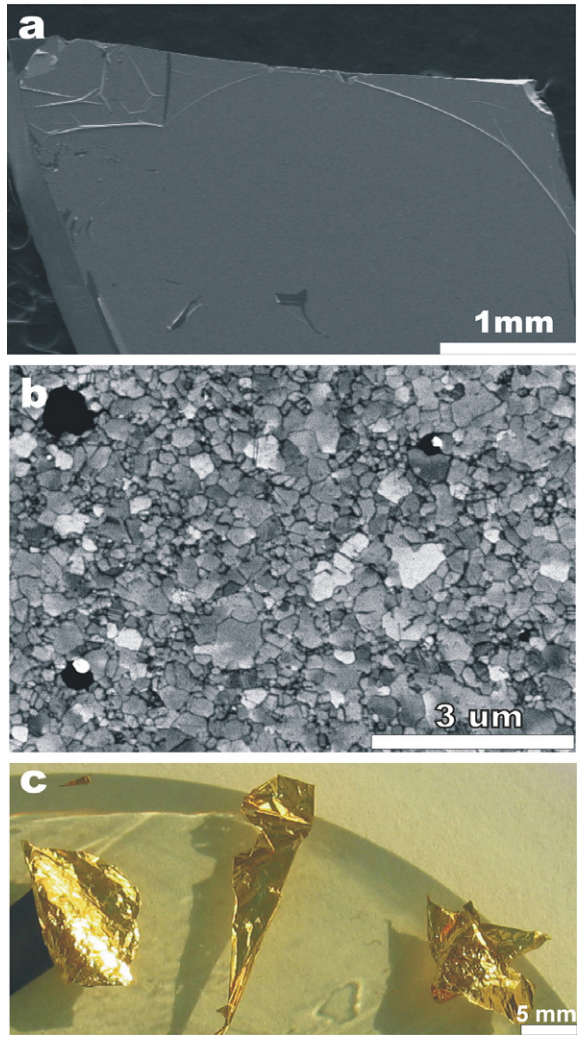

Figure 16. a) SEM image of a Au sample plate on Si substrate after 26 h 35 min treatment in the ethanol solution of 2-PS (8 mM). The beginning of the detaching process can be observed at the upper left-hand corner of the sample. b) Magnification of the upper left-hand corner of image a showing the polycrystalline Au structure similar to the one prior to any treatments. c) Photograph of the ca. 30 nm thick self-supporting gold foil after detaching it from the substrate by ethanol solution of 2-PS.[V]

5.2.2 Graphite

Graphite can have hexagonal or rhombohedral forms which both consist of planar layers of hexagonal nets of carbon atoms. The layers of these forms are arranged in different vertical positions. The distance between the layers is 335.4 pm and the C−C distances within the layers 141.5 pm.[252] Highly oriented pyrolytic graphite (HOPG) is the most popular substrate for liquid-solid interface studies under ambient conditions, since it is electrically conductive, flat, inert and easy to clean.[210] HOPG consists of polycrystals with a lateral grain size typically between 30 nm and 3 mm. The grain size depends on the graphite grade but is large enough to ensure atomically flat surfaces for AFM and STM studies.[253] Therefore, HOPG was selected as the substrate for the 2D metal salophen complex assemblies (Chapter 6.2.3).[VII]

6 Applications of functionalised surfaces

In general, SAMs can be used in a variety of applications, such as chemical sensors,[254-256] electrochemistry,[257] catalysis,[258] and corrosion protection (see Chapter 3.1.2 for examples). In electrochemistry, functionalised SAMs provide fast electron transfer, good selectivity, and high sensitivity to the electrode. In addition, the electrodes are stable with controlled chemical features and well-defined structures.[259] With SAMs the interface and surface properties, such as lubrication,[260,261] adhesion,[262,263] and wetting,[264-266] of the devices can be modified.

However, immobilised metallomacrocycles have been developed for fuel cell applications[267] and a monolayer of bipyridine derivative on Au(111) acts as an effective host to coordinate Pd(II) chloride.[202] The complexation/decomplexation of metal ions on solid surfaces is important for technological applications, such as construction of sensitive, selective, and cost-effective chemical sensors and memories.[202]

6.1 Metal complexes on gold

The motivation for the formation of metal complex SAMs on metal surfaces is their potential technological applications. Thereby, electroactive, chromophoric, and

fluorescent metal complexes are studied extensively, especially on gold surfaces.[268] In this chapter, focus is especially put on the metal complexes suitable for such applications. Efficient film preparation for a specific application requires the use of appropriate molecular functionalities on the metal substrates and in many cases amphifunctional adsorbed molecules are required. One part of such molecules has a strong affinity for metallic surfaces and another part has either weak or no affinity towards the surface. In addition, the terminal functional group of the adsorbate must often have certain specific chemical characteristics.[205,206] Importantly, adsorption of the metal complex on a surfaces does not significantly change the properties of the complex.[269]

Metal complexes can be self-assembled on a gold surface by two different procedures: using a linker molecule or via direct assembly (Figure 17). The linker molecule is applied on the surface, the metal complex added and reacts with the linker. In the direct assembly the ligand must have appropriate functional groups for the attachment and thus this approach normally requires more synthetic work than the linker molecule procedure.[205,268-270] Both these approaches are extensively used and as many different types of metal complexes have been self-assembled on gold surfaces, only some of them can be introduced and discussed in this study. Very often metal complex SAMs on gold surface have been used for electrochemical purposes (see for example ref. 259, 271 and 272) and these are discussed very briefly in this chapter.

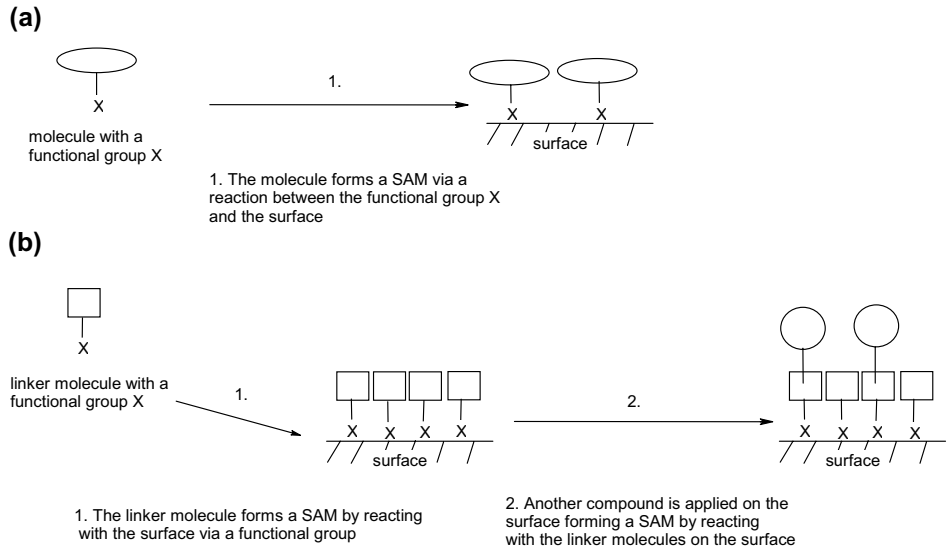

Figure 17. Direct self-assembly (a) and linker molecule (b) approaches for SAM formation.

Metallophthalocyanines have been often arranged on metal surfaces since they have interesting photophysical, electronic, and electrochemical properties. The functionalised surfaces have been used for example as catalysts, photoconductors, gas sensors and in optoelectronic and microelectronic devices.[221,271] Zn(II) phthalocyanines are excellent photosensitisers and they have also been reported as gas sensors. Peripherally with alkanethiols and phenylthiols substituted metallophthalocyanine complexes have promising electrochemical and photochemical properties as electrocatalysts and photocatalysts.[271] Porphyrin SAMs, which are stable and have interesting optical and electronic properties, can be used in catalysis, sensors, and molecular and electronic devices.[222] Thiol-derivatised metalloporphyrin has been reported to chemisorb on a gold surface mostly as a tightly bound, well-defined monolayer but also weak multilayer adsorption has been observed.[259] Besides the above applications, self-assembled structures of porphyrins are attractive in obtaining better understanding of light-energy conversion mechanisms of ordered porphyrins.[222] Yet significant efforts are required in order to obtain organised supramolecular scaffolds with optimum light-harvesting efficiency and transfer rates at the practical level.[273]

In materials research, thin organic, organometallic, and polymer films exhibiting nonlinear optical properties are of prominent current interest. They possess a variety of interesting applications such as polymers with improved nonlinear optical properties and use of single molecules in multilayer systems for thin-film optical devices.[274] So far relatively few nonlinear organometallic materials have been studied. Since many organometallic compounds have conjugated π-electron systems or low-lying charge-transfer states, they possibly have large nonlinear polarisabilities, just as metal salen, salophen, pyridine, and bipyridine complexes have.[274-277] Molecular-based materials in general have many properties, such as faster response time, lower dielectric constant, and better processability as thin-film devices, superior to the properties of inorganic solids that have traditionally been used as nonlinear optical materials.[275]

Besides the most common applications discussed above, metal complex SAMs on gold surfaces have other more rare uses. For example, a gold surface treated with poly(acrylic)acid and iron(III) nitrilotriacetate complex has been used in immobilised metal affinity chromatography to assist mass spectrometric analysis of phosphorylated proteins.[278]

6.1.1 Linker molecule approach

Many chromophores, such as metalloporphyrins, phthalocyanines, and salophens, have been chemisorpted on a gold surface by using thiols as linkers. 4-pyridinethiol (4-PS) is a commonly employed linker and is very often used as a surface modifier.[205,206,234,279,280,IV] The use of modifiers in general is an effective approach for promoting direct electron transfer of redox metalloproteins. The modifier must be bifunctional so that it can adsorb on the surface and interact with the protein.[206]

For example, coordination of Co(II) and Fe(III) porphyrins, as well as Co(II) phthalocyanine on SAMs of 4-PS, 4-aminothiophenol, and diimidazole derivative linker molecules, has been studied by transmission UV-Vis spectroscopy.[279] Ru(IV) porphyrins have also formed SAMs by coordinating to a nitrogen headgroup of thiol SAM. These SAMs were characterised by optical ellipsometry, XPS, STM, grazing-angle FTIR spectroscopy, and visible spectroscopy.[268]

Furthermore, Fe(II) and Ru(II) cyano complexes[205] and substituted Co(salen) complexes (**21** and **45**)[IV] have been assembled on gold via 4-PS linker molecule. The cyano complex SAMs were studied by surface-enhanced Raman spectroscopy (SERS) and electrochemical techniques.[205] In the present studies, unsubstituted Co(salen) was first self-assembled on Au, but this turned out to be impractical due to its rather low solubility. Thus, complex **45** was prepared and its solubility is higher than that of the unsubstituted complex, as intended. However, the introduction of *tert*-butyl substituents changed the dioxygen activation properties more than expected (Figure 11, page 27). The affinity of the new complex for dioxygen was rather poor. Therefore, **21** was prepared and as early as during the synthesis its high affinity for dioxygen was noticed. This complex is soluble for instance in $CHCl_3$, CH_2Cl_2, TCB and DMF but insoluble in alcohols. The Co(salen) **21** and **45** functionalised surfaces were characterised primarily by AFM but the surface with **21** also by XRR.[IV]

Gold surfaces modified with metal complexes can act as sensors, as demonstrated by Co(II) phthalocyanine, which gives linear response to l-cysteine over a fairly wide concentration range (0.28–20 μM). The sensor was prepared by first forming a 2-mercaptoethanol SAM and then attaching a Co complex covalently on it (Figure 18). It is suggested that the Co complex is most probably attached to 2-mercaptoethanol SAM using one of the peripheral substituents, leaving the other three unattached. The surfaces were studied by electrochemical methods.[270]

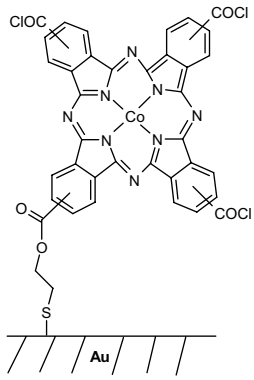

Figure 18. SAM of Co(II) phthalocyanine complex on a gold surface.[270]

6.1.2 Direct self-assembly

An obvious drawback of the direct self-assembly of molecules on surfaces via thiol appendages is the often difficult compound synthesis. In addition, with large, more complex, or charged SAM-forming compounds, the monolayer formation can be poor or totally obstructed. The large systems might not form ordered monolayers due to the covalently attached linker molecule that does not provide a close-packing. Problems with the charged species originate often from the disparity of intermolecular forces present. With some charged systems, molecules do not self-assemble on surfaces despite several free thiol functionalities.[268,269]

Chiral Mn(III), Co(III), and Fe(III) salen complexes have been prepared by complexation of the metal chlorides with ligands which were immobilised on a gold surface. The ligands were functionalised with thio(phenylacetylene)$_n$ substituents (n=1 or 2) and were adsorbed on gold via thiol functionality (Figure 19, page 49). In case of all complexes, the surface coverages were better with the longer thio(phenylacetylene) spacer. The electron-transfer reactions in the monolayers studied by cyclic voltammetry showed reversible redox reactions between M(III) and M(II) for all immobilised complexes.[58] However, Ni(II), Cu(II), and Co(II) salophen complexes with functional sulphur substituents were adsorbed on the surfaces and the ad-layers formed were studied by XPS, SIMS, and grazing-angle FTIR spectroscopy techniques. The results suggest that the alkyl chains are disordered and liquid-like. On the average the molecules are adsorbed on gold via one sulphur group of the molecule.[59]

Several complexes on a gold surface have been tested as sensors. Ni(II) macrocyclic complex having a tetraamine ligand was substituted by a thiol functionality (**E**, Figure 19) after which it self-organised on a gold surface. Sensor activity of the formed SAM was demonstrated for thiocyanate anions and soybean inhibitor trypsin protein molecules by using the surface plasmon resonance (SPR) technique.[281] Fe(II), Ni(II), and Zn(II) porphyrins have been self-assembled on gold via the thiol group (**F**, Figure 19) in order to study by electrochemical measurements the electron transport through the SAM and the influence of the metal ion on the transport.[222]

Bilayered Zr(IV), Ce(IV), and Ti(IV) complexes with hydroxamate groups for metal coordination and disulfide moieties for adsorption on gold, have been prepared and characterised by XPS, ellipsometry, and contact angle techniques.[65] In Co(II), Cu(II), Fe(II), Ni(II), and Zn(II) thiocyanate complexes, two thiocyanate groups out of four were converted to thiolates upon chemisorption on a gold surface (Figure 19). By using different metal ions, the metal ion originating electronic effects in the junction can be distinguished, and the effect of different spin states on molecular conductance can be studied. The functionalised surfaces were characterised by XPS, ellipsometry, and IR reflection spectroscopy.[269] The SAM of Re(I) complex with a bipyridine derivative ligand (Figure 19) was characterised by using SPR spectroscopy, SERS,[282] FTIR spectroscopy, ellipsometry, and contact angle measurements.[274]

Quite intricate structures have been also assembled on gold via direct self-assembly. For example, multilayered thin films consisting of multiple components, one of them being a Cu(II) complex, have been fabricated by repeated sequential depositions. First, an alkanethiol with a functionalised headgroup has been assembled, then a carboxylic acid ligand followed by Cu(II) ion and finally by another molecule of the carboxylic acid ligand having a covalently bonded pyrene. These films are photocurrent-generating and the light absorbing group, pyrene, is noncovalently coupled to a gold surface via metal–ligand complexation (Figure 19). The systems have been characterised by conductivity, impedance, contact angle, and IR measurements.[273]

Even though most of the complexes have been assembled on gold via the thiol head group, one differing example exists showing interesting new prospects for complex assembling on gold and other metal surfaces. In that study, the ligand of Zn(II) porphyrin was functionalised with two COOH-groups (Figure 19). The complex formed a stable SAM so that one of the acid groups was bound to gold and the other one formed a

hydrogen bond with an adjacent complex molecule. It is suggested that the porphyrin plane is tilted relative to the gold surface. The interaction between the surface and the assembled molecule is rather weak, and similar interactions could be achieved by employing for example polar COOH or NH_2-groups.[224]

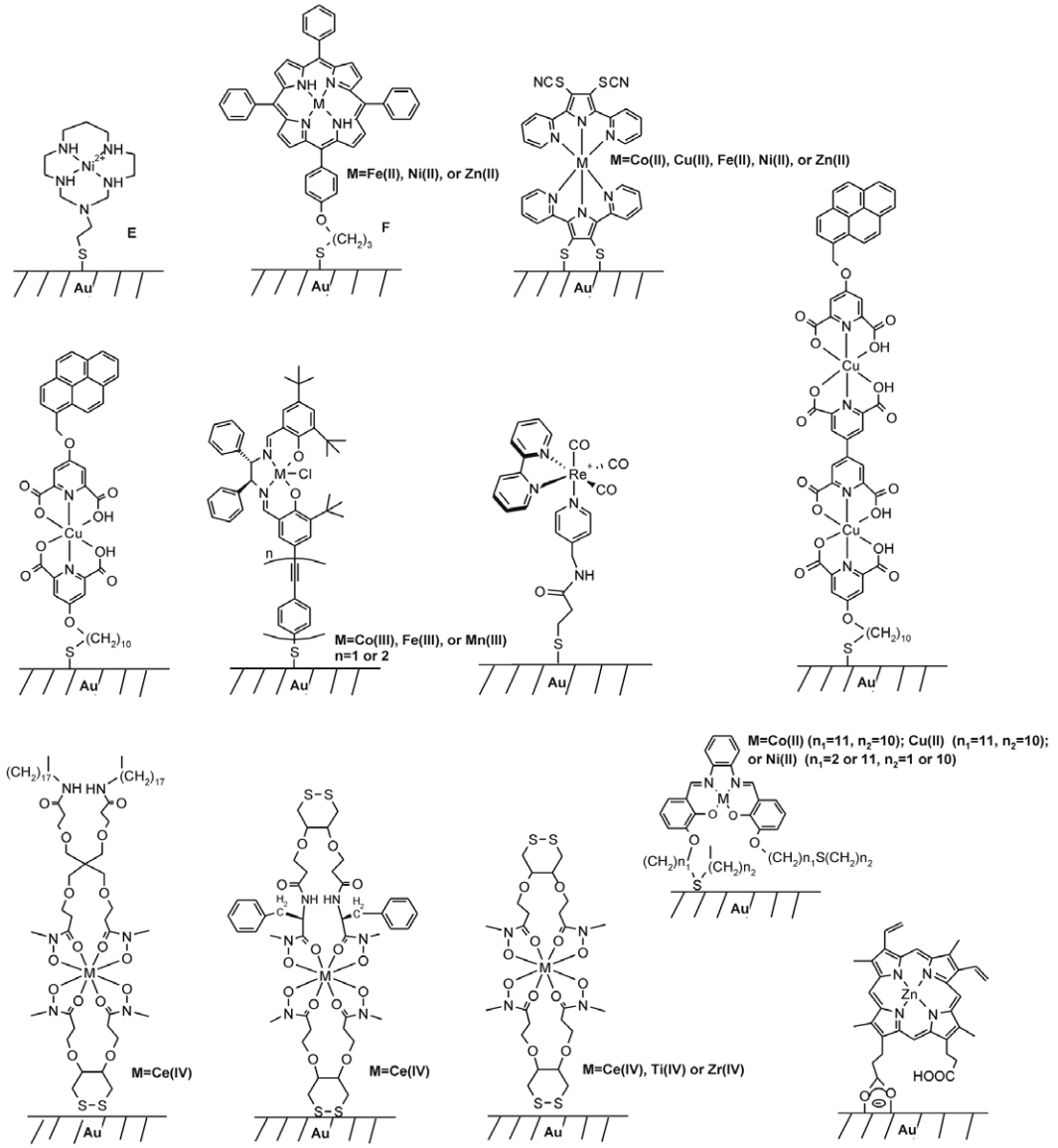

Figure 19. Schematic presentations of the metal(II) complexes self-assembled on gold surface via the thiol functionality of the ligand.[58,59,65,222,224,269,273,274,281]

6.2 Metal complexes on graphite

Typically, compounds must have long alkyl chains for lateral immobilisation of the molecules on HOPG which further facilitates their imaging.[211] Alkyl chains aid in stabilising the SAM since they have high affinity for graphite and the van der Waals interactions between the alkyl chains provide additional stabilisation.[210,219] Assemblies of organic compounds on a liquid-graphite interface or on HOPG (this acronym refers hereafter also to liquid-HOPG interface) have been studied intensively by STM over a decade. The aim has been to understand their formation and thus provide industrial and technological applications such as molecular electronic devices and corrosion protection.[283] In the case of SAMs of metal complexes on HOPG the situation is just the opposite; research has begun only recently to raise interest, and much basic research is needed for understanding all the phenomena governing the formation of the structures. The 2D structures of metal complexes on graphite provide a platform for highly ordered metal decorated surfaces which are needed e.g. in functional nanodevices and for data storage. With minor modifications to the ligands, variation of the alkyl chain length, the distances between the metal centres and hence the metal ion density on the surface can be fine-tuned.[60,61,284,VII]

6.2.1 General considerations

STM is used to study 2D structures of compounds on HOPG because it provides submolecular resolution and can operate in solutions. Aromatic parts of the molecules appear in STM images brighter than alkyl chains due to their higher electron density.[61,192,285,286] A typical physisorbed molecule is highly insulating: the energy difference between the highest occupied molecular orbital HOMO and the lowest unoccupied molecular orbital LUMO is in the range of 10-12 eV (Figure 20). Therefore, the adsorbate film must be thin enough to allow electrons to tunnel between the tip and the substrate.[287] However, it has also been claimed that the film thickness is not critical since the tip penetrates through the excess insulating organic compound.[210] As the diameter of the adsorbed molecules increases, a loss in the resolution follows. Typical tunnelling parameters used in imaging adsorbates are selected so that the gap resistance is in the order of 10^9-10^{10} Ω ensuring that the images are dominated by the features of the adsorbed

molecules and not by the features of the substrate. This also helps to avoid disturbance of the molecules physisorbed at the liquid-solid interface by the tip.[287]

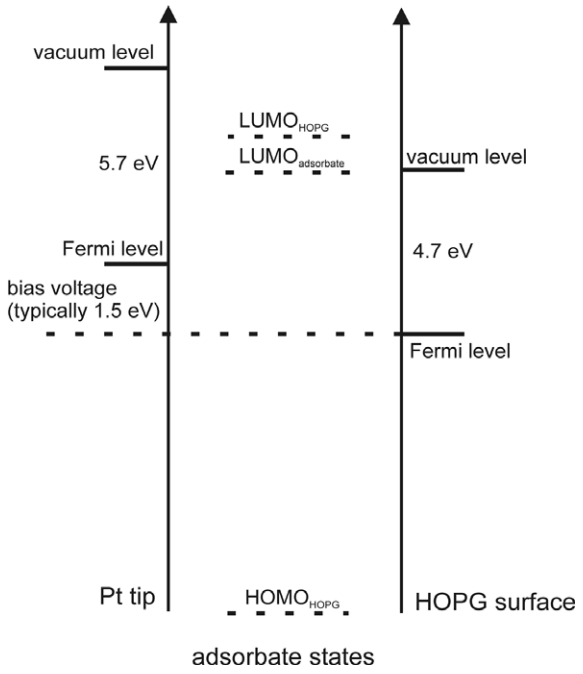

Figure 20. A qualitative energy level diagram of a molecular adsorbate on HOPG with a typical HOMO-LUMO gap of 10-12 eV. Organic molecules are normally insulators and the location of the HOMO and LUMO in the tunnel junction is not well defined. However, the adsorbate energy levels should be several electron volts above the HOPG substrate and Pt tip Fermi levels.[287]

Typical adsorbate molecules are large enough to produce only slow thermal motion within the film at room temperature, so they remain on the surface a sufficient length of time to be imaged. Energetics favour molecule migration to the liquid-solid interface, yet evidence of dynamic motion has been observed, suggesting that the molecules move freely, though slowly, between the surface and the solution. The presence of solvent has a significant effect on the adsorption/desorption dynamics.[287]

Sample preparation in general for STM studies on liquid-HOPG interfaces is straightforward but few requirements for the solvent exist. First, the solvent must be nonpolar so that the tunnelling current can be measured while the tip is under solution. In polar solvents, the ionic current caused by the dissolved ions can be sufficiently large to prevent detection of the tunnelling current. In addition, the solvent must have sufficiently

low vapour pressure to not evaporate during image acquisition. Finally, the solvent must have lower affinity for the surface than the adsorbate of interest thus preventing adsorbate displacement from the surface by the solvent molecules.[287]

A saturated solution of the studied compound is prepared in a non-conducting solvent and then a drop of this solution is introduced on a freshly cleaved HOPG. Good solvents for such purposes are trichlorobenzene, dichlorobenzene, phenyloctane, and 1-octanol. During STM measurements, various types of artefacts can appear (Chapter 4.3) and therefore it is always crucial to repeat the measurements using different HOPGs and tips.

6.2.2 Literature survey of complexes used

Lamellar structures are so far the most common 2D structures reported for metal complexes on HOPG. There are several STM studies where the 2D assemblies of phthalocyanine metal complexes on HOPG have been studied (for applications see Chapter 6.1). For example, Pr(IV) bis-octakis(octyloxy) phthalocyanine forms two different adlayer structures, four-fold and six-fold domains, four-fold being the dominating structure. In both structures, it is proposed that the alkyl chains interdigitate between the neighbouring molecules.[221] Cu(II) phthalocyanine (Figure 21, page 54) has the same octaalkoxyl-substituted phthalocyanine ligand as the aforementioned Pr complex, and it forms the four-fold and six-fold structures coexisting on the surface. It has been suggested that in the four-fold symmetrical structure the molecule−substrate interactions are relatively weak but in the six-fold structure strong molecule−substrate interactions dominate.[211] In addition to plain complexes, co-adsorption of Cu(II) and Pr(IV) phthalocyanines with different organic compounds on HOPG have been studied.[217,221,288-290]

Many unbridged Schiff base complexes (Figure 21, page 54), mostly with Cu(II), have been studied on HOPG but mainly by one research group. Rieger *et al.*[60,61] have prepared a systematic series of Cu(II) and Pd(II) aldiminato complexes, where the position and length of the alkoxy or alkyl chains have been changed. Variations in the ligand structure provided fine-tuning of the thirteen, virtually lamellar, structures.[60,61] Qian *et al.* have determined 2D structure of *in situ* complexed bis(*N*-octadecylsalicylaldimine)Cu(II). The complex took a *trans*-configuration and arranged in a lamellar structure where the

alkyl chains of the molecules from neighbouring lamellae were fully interdigitating. The structure obtained was similar to the structure of synthesised pure Cu complex thus confirming successful *in situ* complexation.[62] Prior to these studies,[VII] only one bridged Schiff base complex, (bis(5-dodecylsalicylidene)ethylene-diaminato)Ni(II) (Figure 21), had been imaged on HOPG by STM. It had been suggested that the complex formed dimers, and that the alkyl chains showed no apparent interaction with other parts of the molecule but that they seemed to lie over the HOPG surface.[63]

Zn(II), Ni(II), and Rh(III) porphyrin complexes (Figure 21) have been studied on HOPG for the same reasons as on a gold surface (Chapter 6.1).[291-293] With Zn and Ni porphyrin complexes, it has been shown that such surfaces can be imaged by chemically modified STM tips. First, the STM images were obtained with unmodified tips and Zn and Ni centres appeared as dark depressions. When the 4-PS modified gold tip was used, the metal centres occurred as bright spots. This is suggested to be due to metal coordination interactions between the central metal and the pyridyl group of the 4-PS on the gold tip. These interactions probably modify the overlap of the local density of states of the sample and tip, resulting in increased tunnelling current.[291]

To further demonstrate the improved contrast variations achieved in STM images with 4-PS modified tips, the mixture of pure ligand and Zn porphyrin as well as the mixture of Zn and Ni porphyrin complexes were studied. In the former case, two kinds of bright spots were observed. The moderately bright spots were suggested to be the centres of the pure ligand and the very bright spots the metal centres. In the case of the mixture of Zn and Ni complexes moderately and very bright spots were obtained. By changing the ratio of the complexes, the very bright spots could be assigned to Zn centres and the other spots to Ni centres.[291]

The effect of the tip-to-sample distance on the contrast variations of the STM images was examined with bis[1,3-di(*p*-*n*-tetradecyloxyphenyl)propane-1,3-dionato]Cu(II) (Figure 21). The STM image was obtained with a high resolution showing the separation between the alkyl chains and the metal-containing core. With various tunnelling currents (bias voltage was kept constant), the image features of the core parts of the molecules differed remarkably whereas the appearances of the alkane chains were almost the same. The molecular core contribution was suggested to dominate the image contrast.[294]

Alkyl chain length change alone can affect imaging of the structure, as was found for two porphyrin Rh(III) chloride complexes having coordinated pyridine (Figure 21).

The complex with triacontyl groups, Rh(C_{30}OPP)(Cl)(py), was imaged from pure solvent, whereas the complex with octadecyl groups could be imaged clearly only from a solution containing a mixture of the complex and a free ligand. However, even in the best case the images were only molecularly resolved and therefore molecular structures were not proposed for the 2D assemblies. It was suggested that the longer alkyl chains leading to higher adsorption energy contributed to the formation of the Rh(C_{30}OPP)(Cl)(py) SAMs from plain solvent. Furthermore, the high adsorption energy of Rh(C_{30}OPP)(Cl)(py) should hinder the molecular exchange between the SAM and the supernatant.[292]

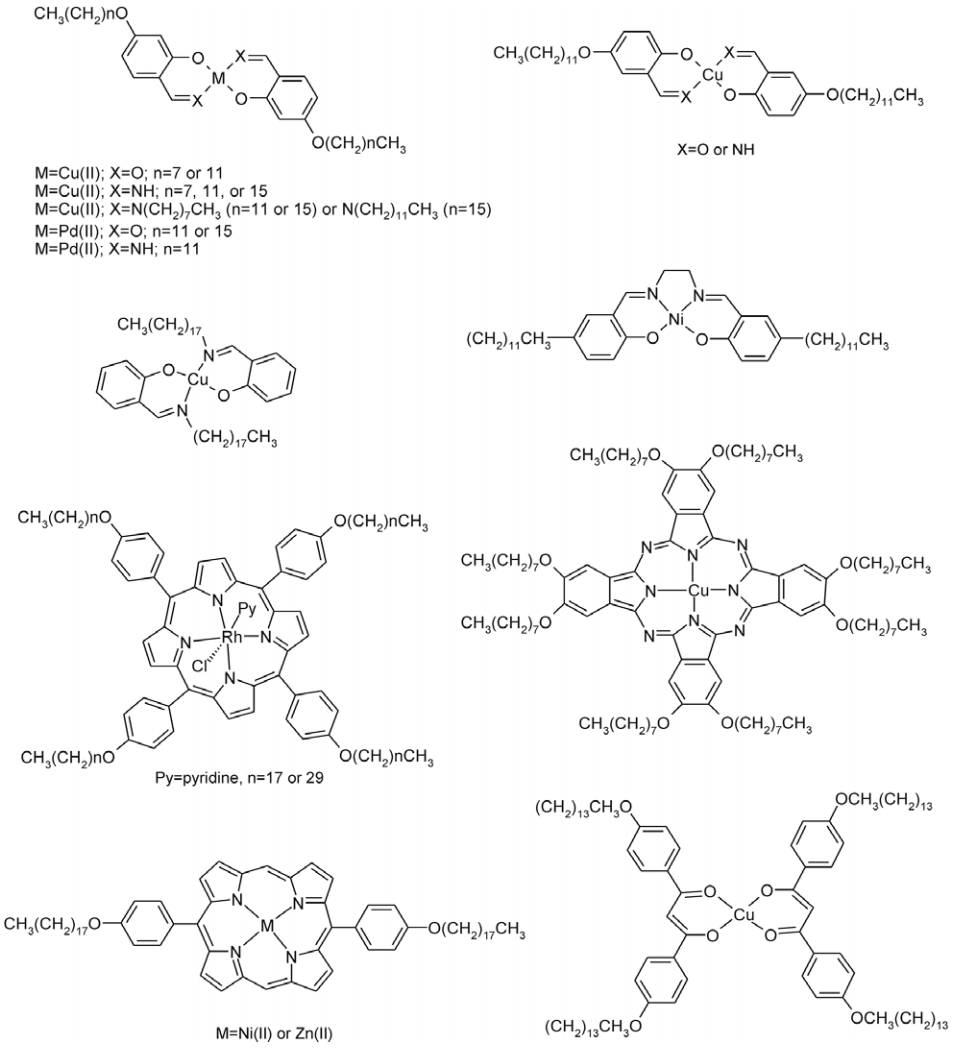

Figure 21. Selection of metal complexes studied on HOPG.[60-63,211,291,292,294]

An interesting aspect was noted in the studies of two ferrocene (Fc) complexes having long alkyl chains, when comparing their adlayers on HOPG with their single crystal structures.[295,296] Oligomethylene bridged diferrocenes with the structure Fc–$(CH_2)_n$–Fc or Fc–$(CH_2)_n$–CH=CH–$(CH_2)_n$–Fc formed lamellar structures. The lamellae consisted of parallel double rows of closely neighbouring Fc end groups separated by maximally extending parallel oligomethylene (–CH_2–)$_n$ spacers.[296] In the 2D pattern of tetradecylferrocene, Fc$(CH_2)_{13}CH_3$, the C_{14}-sidechain was in the maximally extended form with all saturated hydrocarbyl subunits and alkyl chains fully interdigitating.[295]

Besides the complexes described above, many grid-type metal complexes with four metal centres have been studied and some of them have shown different morphologies on HOPG.[219,220,297] Cu(II) and Pd(II) complexes with modified 2,2'-bipyridine ligands have been also studied together with Pd(II) bis(β-diketonate) complexes.[214,284,298] Even though for the bis(β-diketonate) complexes no images with submolecular resolution have been attained, it is suggested that the alkyl chains of the adjacent molecules interdigitate.[214,284]

6.2.3 Metal salophen complexes

The aim of this study was to obtain understanding on formation of 2D structures of metal complexes on HOPG. For such studies, a series of metal salen and salophen complexes were prepared (Figure 6, page 20). Complexes with different metal centres and alkyl chain lengths that were substituted symmetrically or unsymmetrically were synthesised. Possible differences in the assembling of ligands and metal complexes were also of interest.[VII]

From the measurements carried out in the constant-current mode, several important features were observed. Most importantly, even relatively small changes in the ligand or change of the metal ion can significantly affect the SAM formation and the 2D patterns. As an example, STM images were obtained only for salophen (phenylene-bridge between the imino nitrogens) complexes, not for salen (ethylene-bridge or tetramethylated ethylene-bridge) complexes.[VII] Attempts to study the effect of symmetrical alkyl chain substitution vs. unsymmetrical substitution also failed, since STM images were only obtained for one symmetrically substituted salen complex with ester chains, though not with high resolution (Figure 22).

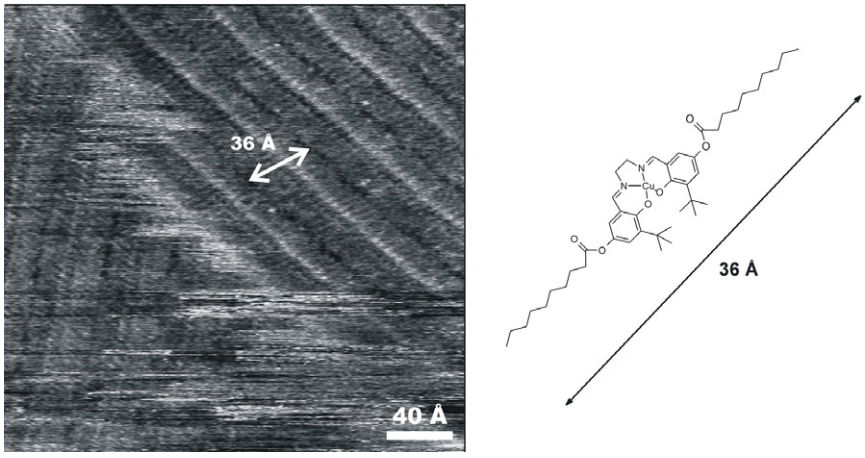

Figure 22. STM-image of Cu(II) complex **46** and the proposed structure. Due to the low image resolution, it is not possible to provide the detailed molecular arrangement.

A clear difference in the imaging of salophen complexes and ligands was also observed. All prepared complexes except those of Fe(II) formed reproducible SAMs within minutes after introducing the sample solution on HOPG, but the images were obtained only for the salophen C_{12}-ligand (Figure 23).[VII]

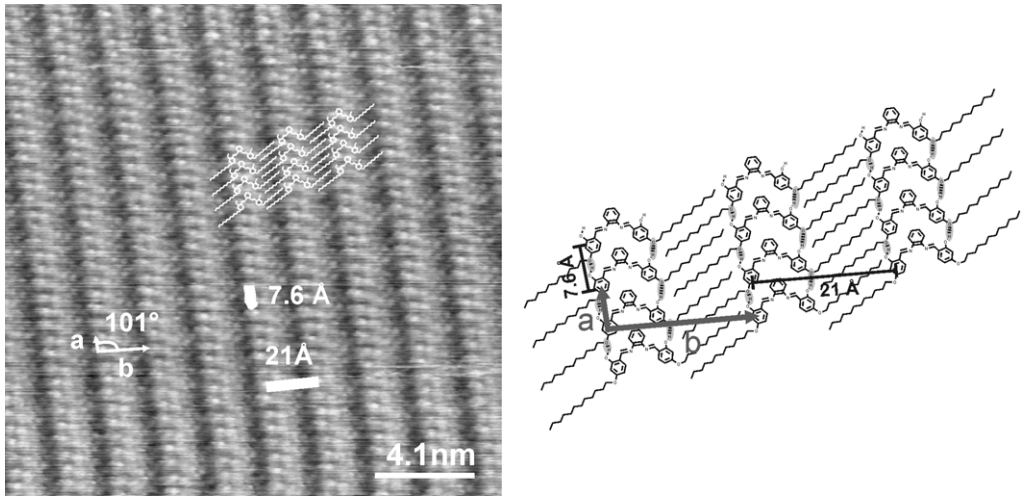

Figure 23. High-resolution STM image (left) and the proposed molecular model (right) of the salophen C_{12}-ligand on HOPG. Image area 203 Å×203 Å, U_{set}=-259 mV, I_{set}=18.2 pA. Unit cell dimensions: a=7.6±0.2 Å; b=21±0.2 Å, angle 101±2°. The hydrogen bonding of molecules is shown by the dotted lines and the grey overlay.

It was attempted to image salophen complexes with hexyloxy side chains but without success. In addition, images were not obtained for Fe(II) salophen complexes as for equivalent Cu, Co, and Ni complexes. It is proposed that Fe complexes and complexes with C_6-chains, as well as salophen ligands with shorter alkyl chains (C_{10} or less) and salen complexes are too mobile on HOPG for successful STM imaging. It has been previously reported that even if the molecules are easily adsorbed on the surface, obtaining high-resolution images may be difficult due to mobility of the molecules within the basal plane. Furthermore, the scanning tip may introduce perturbance that interferes with imaging.[211] In the case of Fe(II) complexes, it is likely that they form rather fast μ-oxo complexes when in contact with air and thus they are not sufficiently planar for STM-imaging.[299] Salen complexes also seem to be too non-planar, as they often favour umbrella or stepped conformation instead of planar which is common for salophen complexes (Chapter 3.2.2).

6.2.3.1 Parallelogram-like structure

The Cu complex with C_8 alkyl chains (**37**) formed a parallelogram-like structure (Figure 24). In this assembly, every second complex molecule within a lamella is twisted by 18° with respect to the preceding molecule. As a consequence, this kind of assembly can be visualised as an array of almost individual parallelograms. The periodicity of the lamella is reflected by the metal−metal distance along the *b*-axis (17±0.2 Å). The intermolecular metal–metal distances within a lamella alternate between 12±0.2 Å (*b*-axis) and 17±0.2 Å (*a*-axis). Interdigitation of the alkyl chains varies in the assembly and one molecule within a parallelogram acts like a glue between the individual parallelograms. Three other molecules within a parallelogram have relatively weak van der Waals forces. Additional $C_{Ar}H\cdots O_{alkoxy}$ hydrogen bonds[300] with a distance of 2.7±0.2 Å provide stabilisation for the structure.[VII]

The parallelogram-like structure was obtained also for Co and Ni complexes **29**, **30**, **33**, and **34** with C_8 and C_{10} alkyl chains (Table 4). Although the image resolution of these complexes does not facilitate interpretation of the 2D fine-structure, it is clear that an alkyl chain length and metal ion interplay exists in the formation of these structures.[VII]

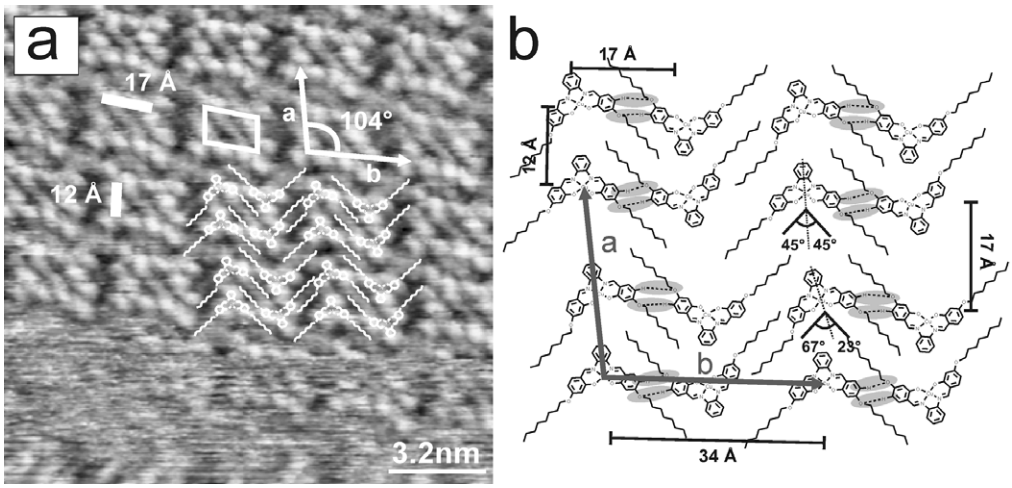

Figure 24. a) High resolution STM image of complex **37**, area 161 Å × 161 Å, U_{set}=-630 mV, I_{set}=29.3 pA. b) Proposed molecular model. Unit cell dimensions: a=28.5±0.2 Å, b=34.0±0.2 Å, angle 104±2°. The hydrogen bonding in a parallelogram is shown by the dotted lines and the grey overlay.[VII]

Table 4. Unit cell dimensions of salophen complexes **29**, **30**, **33**, **34** and **37**.

Complex	**Unit cell**		
	***a* (Å)**	***b* (Å)**	**angle (°)**
CuC_8 (**37**)	28.5±0.2	34.0±0.2	104±2
NiC_{10}(**34**)	28.0±0.2	28.0±0.2	90±2
NiC_8 (**33**)	25.0±0.2	27.0±0.2	95±2
CoC_{10} (**30**)	28.0±0.2	33.5±0.2	92±2
CoC_8 (**29**)	22.0±0.2	34.0±0.2	100±2

6.2.3.2 Honeycomb structure

Co(II) and Ni(II) complexes (**31** and **35**) bearing the same C_{12}-ligand as **39**, formed honeycomb-type network patterns consisting of hexagons of six molecules (Figure 25). A structural model where each molecule has three nearest neighbours within a range of 12-15±0.2 Å is proposed. The alkyl chains of each molecule are parallel to the bisector of the salophen complex and perfectly interdigitate with those of the opposite molecule within a hexagon. Besides the van der Waals forces between the alkyl chains, the pattern is

stabilised by intermolecular $C_{Ar}H\cdots O_{alkoxy}$ hydrogen bonds (*ca.* 2.6±0.2 Å) and every molecule has two of these.[VII,300]

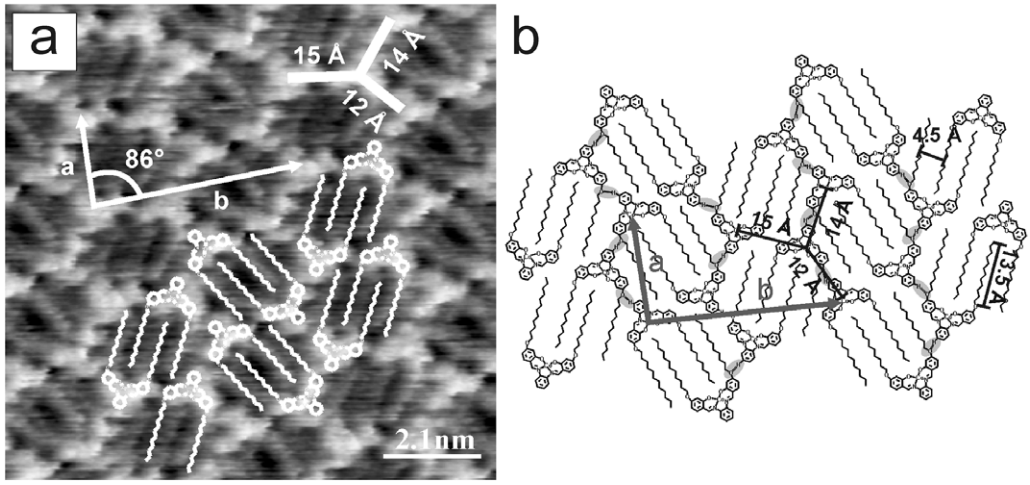

Figure 25. a) High resolution STM image of complex **31** with an image area of 104 Å×104 Å, U_{set}=-180 mV and I_{set}=12.8 pA. b) Proposed 2D structural model. Unit cell dimensions: a=19.5±0.2 Å, b=46.0±0.2 Å, angle=86±2°. The hydrogen bonding in a honeycomb is shown by the dotted lines and the grey overlay.[VII]

6.2.3.3 Twisted structure

Cu complexes **38** and **39** with long alkyl chains, C_{10} and C_{12} respectively, formed reproducibly twisted structures (Figure 26). Even though the STM image of **38** was obtained with a high resolution, the resolution in some parts of the image is not high enough to allow a fully unambiguous structural characterisation. In the model suggested, the molecules are arranged in a way that the alkyl chains and aromatic parts of the molecules alternate, which can be illustrated as kind of lamellae. Here, the lamellae constitute of a repeating unit of two molecules, and the neighbouring lamellae are dissimilar. The measured lamellar periodicities for **38**, 22.0±0.2 and 27.5±0.2 Å, suggest interdigitation between the alkyl chains of neighbouring lamellae.[301] The observed distances between the alkyl chains vary rather much (3.7±0.2 Å, 4.1±0.2 Å, 4.3±0.2 Å and 6.3±0.2 Å) within the ordered structure and all distances, except the longest, are rather typical of close-packed alkyl chains.[301,302] Besides the van der Waals interactions between the alkyl chains, the $C_{Ar}H\cdots O_{alkoxy}$ hydrogen bonds (2.4±0.2 Å and 2.6±0.2 Å) stabilise the

pattern.[300] The shortest metal–metal distances (10±0.2 Å) in the pattern are the distances within a lamella. When the alkyl chain length is increased from C_{10} (**38**) to C_{12} (**39**), the periodicity of the lamellae is augmented to coincide with the longer alkyl chain length.[301] This augmentation was expected and facilitates fine-tuning of the 2D structure.[60]

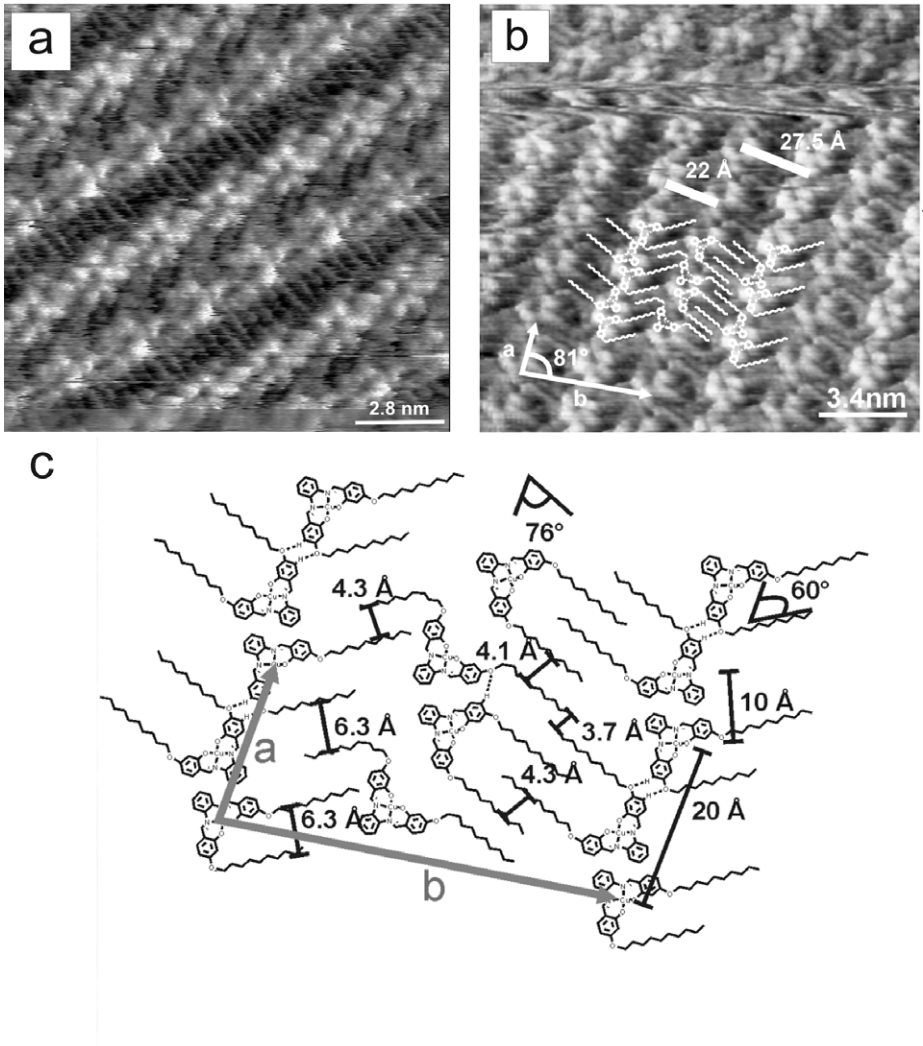

Figure 26. High-resolution images of complex **38** with an image area of a) 146 Å×146 Å, U_{set}=-880 mV, I_{set}=9.21 pA and b) 170 Å×170 Å, U_{set}=-108 mV, I_{set}=32.2 pA. c) Proposed molecular model. Unit cell dimensions: a=20.0±0.2 Å, b=49.5±0.2 Å, angle=81±2°. STM image of **39** at the liquid-HOPG interface shows the same features as **38** but with a longer periodical distance.[301]

6.2.3.4 Origin of different 2D structures

As shown above, the 2D structures of complexes on HOPG can be affected by the choice of the metal ion and the alkyl chain length (Figure 27). It is suggested that the driving force for the assemblies is a subtle interplay between a maximum amount of attractive van der Waals interaction of the alkyl chains and weak hydrogen bonds on the other side. In each particular case, the global energetic minimum is reached by a compromise between these interactions.[VII,301]

In the twisted structures of Cu(salophen) complexes **38** and **39** (alkyl chain length C_{12} and C_{10}, respectively), van der Waals interactions between the alkyl chains and $C_{Ar}H\cdots O_{alkoxy}$ hydrogen bonds are the stabilising forces. In the parallelogram-like pattern of the CuC_8 complex (**37**), the van der Waals interactions are weaker than in **38** and **39** but this is compensated by $C_{Ar}H\cdots O_{alkoxy}$ hydrogen bonds. Co and Ni complexes with C_{12} alkyl chains seem to favour the maximum possible number of hydrogen bonds to stabilise their honeycomb assemblies, taking into account that there is always a compromise between the van der Waals forces and hydrogen bonds. The observed structural differences in the 2D morphologies could be due to electronic effects that may influence the intermolecular interactions, such as hydrogen bonds, and therefore the packing.[VII,301]

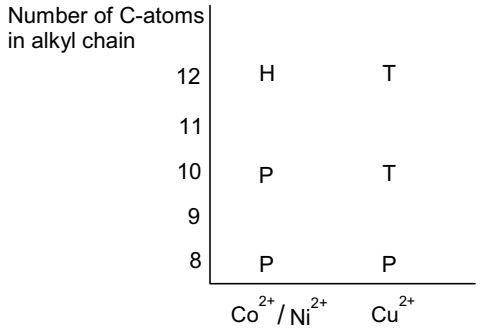

Figure 27. A diagram showing the effects of alkyl chain and metal ion on the 2D pattern. H = honeycomb, P = parallelogram-like and T = twisted structure.[VII, 301]

Average metal ion coverage on the surface, and therefore the metal–metal distances, are important for the metal-ion patterning of the surface. From the three structures obtained, the twisted assembly provides the shortest (10±0.2 Å) metal–metal distances. However, due to more separated aromatic and alkyl chain parts compared with

the other two structures, the average metal ion coverage is only *ca.* 0.40 metal ions/nm^2 (estimated from 5 nm×5 nm area). For honeycomb and parallelogram-type structures the equivalent value is slightly higher, *ca.* 0.48 and 0.52 metal ions/nm^2, respectively.[VII, 301]

6.2.3.5 Comparison of 2D and 3D structures

Comparison of 2D and 3D structures of compounds is important as it helps to gain understanding of self-assembly processes in crystals and on surfaces.[303] This, on the other hand, is of utmost importance as the prediction and design of 3D crystal structures still remains challenging.[304] Furthermore, knowledge of the real surface structure of compound is crucial from the application point of view as orientation and relative position of the molecules are important for tailoring desired properties.[67] High resolution STM images with visible sub-molecular features require often much efforts whereas in other cases single crystals suitable for X-ray crystallography are difficult to obtain. Therefore, depending on the compound, it would be very convenient if the 2D pattern could be deduced from the 3D structure or vice versa.

Several studies on 2D vs. 3D packing of different organic compounds suggest similarity of these packings[303,305-308] but also opposing studies exists.[308-310] On the contrary to organic compounds, studies combining the 2D and 3D structures of metal complexes are rare. Only very recently Wedeking *et al.*[295,296] have compared the 2D adlayers of two ferrocene (Fc) complexes, namely Fc–$(CH_2)_{14}$–Fc and Fc$(CH_2)_{13}CH_3$, on HOPG to their single crystal structures. In both 2D/3D systems, the characteristics of the physisorbed patterns on HOPG could be deduced from their 3D packing diagrams.[295,296]

As already mentioned in Chapter 3.2.2, single crystals of salophen complexes with long alkyl chains (C_8-C_{12}) could not be obtained despite numerous efforts. However, crystal structures of equivalent Cu(salen) complexes were obtained relatively easily, whereas their 2D patterns remained unattained. However, it can be assumed that single crystal structures of analogous salen and salophen complexes are not significantly different in terms of the molecular packing. Therefore, we compared molecular packings of Cu(II) salen complexes (**25**-**27** and **27·MeOH**) bearing long (C_8-C_{12}) alkyl chains to the 2D patterns of equivalent Cu(II) salophen complexes (**37**-**39**).[III,VII,301]

In the 3D structures of **25**-**27** (Figure 28, page 64), the minimum C−C distances between the alkyl chains were in the range of van der Waals interactions, *ca.* 3.80-4.46 Å,

and besides these interactions, numerous CH···O hydrogen bonds provided stabilisation. When the 3D structures are compared to the 2D assemblies of **37**-**39**, it can be noticed that they provide closer packings and have more stabilising forces than the 2D patterns (Chapters 6.2.3.1-6.2.3.4). Furthermore, it is very important to notice different effects that possible axially coordinated solvent molecules induce on 2D and 3D structures. As the structures of complexes **27** and **27·MeOH** show, the solvent molecule can change the packing in 3D structures significantly.[III,VII,301] On the contrary, in 2D assemblies the axial solvent molecule would be most likely to point into the solution and it would not have any effect on the pattern formation.

Two different 2D structures, both with interdigitating alkyl chains, can be constructed from the 3D structures of **25**-**27** (Figure 29, page 65). They would appear with equal probability on the substrate and it cannot be predicted which one of them would be actually formed. Furthermore, alkyl chain length has no influence on the resulting structures in contrast to the imaged 2D patterns of **37**-**39**. Finally, the derived structures are not the same as imaged with **37**-**39**. Thus, it is suggested that in the case of the complexes studied, 2D assemblies cannot be derived in detail from the molecular crystal packing of the complexes. Presumably, the adsorbate−substrate and van der Waals interactions together with possible hydrogen bonds create such a complex system in which the pattern formed on HOPG is a compromise between all these forces.[III,VII,301]

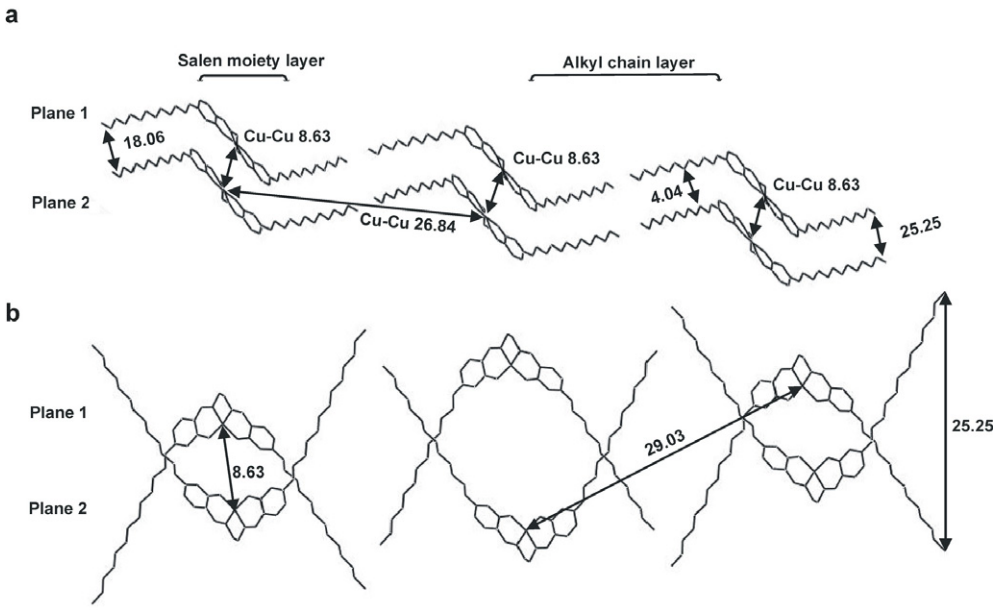

Figure 28. a) Crystal packing of complex **27** viewed from the angle showing the "lamellar" structure. The alternating structure of the alkyl chains and salen moieties is visible. b) Crystal packing of **27** from another angle showing more clearly that the molecules within the "lamella" are in different planes. The distances between the alkyl chains and Cu ions are in ångströms and the hydrogen atoms have been omitted for clarity. Complexes **25** and **26** are packed similarly to **27**. In **25** the corresponding Cu–Cu distances as shown in Figures a and b are 8.412, 14.936, and 22.023 Å, and in **26** 8.245, 14.662, and 24.908 Å.[III]

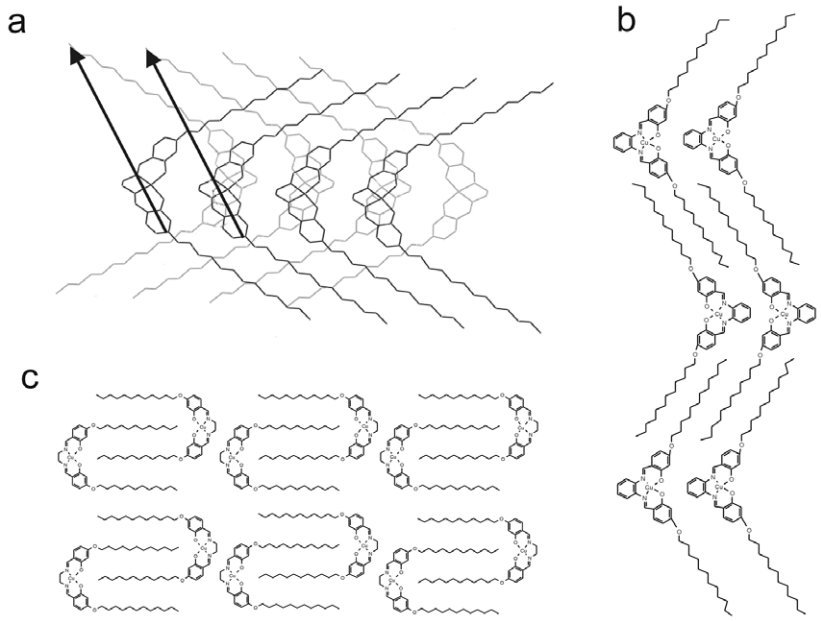

Figure 29. Construction of 2D patterns from the 3D structure of complex **27** assuming that in the 2D structure the molecules are planar and the closest possible packing results. a) The two different planes are shown in black and grey. When all molecules shown in black are moved into the analogous positions, indicated by the black arrows, a lamellar structure with fully interdigitating alkyl chains is achieved. b) Schematic model of the 2D lamellar structure with interdigitating alkyl chains of the neighbouring lamellae. c) Schematic model of another pattern which can be derived from the 3D structure. For complexes **25** and **26** the 2D patterns are obtained similarly.[III]

7 Concluding remarks

In this study, two-dimensional assemblies of cobalt, copper, iron, and nickel salen and salophen complexes were of interest. In order to study the patterns they form on liquid-graphite interface and on polycrystalline gold surface, the ligand precursors and metal complexes were synthesised and fully characterised. In addition, several new solid state structures were obtained and the dioxygen coordination properties of different cobalt complexes were studied by UV-Vis spectroscopy. The imaging of self-assembled monolayers by AFM and STM techniques requires smooth surfaces, and therefore significant efforts were made to find the proper structures for gold thin film substrates.

Co(salen) complexes were arranged on a gold surface by using 4-pyridinethiol as a linker molecule. As a side-product of these studies, a new thiol-assisted procedure for oxidation of solid gold was found and by altering the reaction conditions preparation of

thin gold foils (30 nm thick) became feasible. In addition, coordination of pyridinethiols on Au(I) was studied in more detail.

The STM studies of cobalt, copper, and nickel salophen complexes revealed three new 2D patterns illustrating the previously unreported interplay between the alkyl chain length and metal ion and showing its effect on the formation of these patterns. Furthermore, the specific requirements that the studied complexes and ligand precursors must fulfil prior to successful imaging on liquid-graphite interface could be illustrated. As the three different 2D patterns obtained and their comparison to single crystal structures of analogous Cu(salen) complexes hint, in this particular case it is not likely that the 2D structures can be derived from the 3D single crystal structures. This is due to the relatively complex system where the optimum pattern is formed as a compromise between van der Waals interactions, intermolecular hydrogen bonds and adsorbate-substrate interactions.

Further studies could be to continue examination of the 2D structures of metal complexes on different substrates but more importantly to examine applications such as catalysis or molecular level sensors. The substrates of main interest would be both gold and liquid-graphite interface but also silicon. It would be beneficial to study whether the highly-ordered 2D patterns of salophen complexes formed on liquid-graphite interface survive on graphite after removal of the solvent. If they survive, the organic parts of the complex molecules could be removed and the sites of the metal centres formed could be located.

References

(1) Schiff, H. *Ann.* **1864**, *131*, 118.

(2) Schiff, H. *Ann. Chem. Suppl.* **1864**, *3*, 343.

(3) Schiff, H. *Ann. Chem.* **1869**, *150*, 193.

(4) Schiff, H. *Ann. Chem.* **1869**, *151*, 186.

(5) Cozzi, P. G. *Chem. Soc. Rev.* **2004**, *33*, 410−421.

(6) Garnovskii, A. D.; Nivorozhkin, A. L.; Minkin, V. I. *Coord. Chem. Rev.* **1993**, *126*, 1−69.

(7) Fiammengo, R.; Bruinink, C. M.; Crego-Calama, M.; Reinhoudt, D. N. *J. Org. Chem.* **2002**, *67*, 8552−8557.

(8) Pui, A.; Berdan, I.; Morgenstern-Badarau, I.; Gref, A.; Perrée-Fauvet, M. *Inorg. Chim. Acta* **2001**, *320*, 167−171.

(9) Pui, A.; Berdan, I.; Caşcaval, A. *Rev. Roum. Chim.* **2000**, *45*, 331−335.

(10) Larrow, J. F.; Jacobsen, E. N. *Top. Organomet. Chem.* **2004**, *6*, 123−152.

(11) Sun, W.; Wang, H.; Xia, C.; Li, J.; Zhao, P. *Angew. Chem., Int. Ed.* **2003**, *42*, 1042−1044.

(12) Katsuki, T. *Adv. Synth. Catal.* **2002**, *344*, 131−147.

(13) Katsuki, T. *Coord. Chem. Rev.* **1995**, *140*, 189−214.

(14) Cai, L.; Mahmoud, H.; Han, Y. *Tetrahedron: Asymmetry* **1999**, *10*, 411–427.

(15) Drozdzak, R.; Allaert, B.; Ledoux, N.; Dragutan, I.; Dragutan, V.; Verpoort, F. *Adv. Synth. Catal.* **2005**, *347*, 1721–1743.

(16) Liu, S.-Y.; Nocera, D. G. *Tetrahedron Lett.* **2006**, *47*, 1923–1926.

(17) Meng, X.-G.; Zhu, J.; Yan, J.; Xie, J.-Q.; Kou, X.-M.; Kuang, X.-F.; Yu, L.-F.; Zeng, X.-C. *J. Chem. Technol. Biotechnol.* **2006,** *81***,** 2–7.

(18) Wang, Y.; DuBois, J. L.; Hedman, B.; Hodgson, K. O.; Stack, T. D. P. *Science (Washington, DC, U.S.)* **1998**, *279*, 537–540.

(19) see for example Kervinen, K.; Korpi, H.; Leskelä, M.; Repo, T. *J. Mol. Catal. A: Chem.* **2003**, *203*, 9–19.

(20) Chaube, V. D.; Shylesh, S.; Singh, A. P. *J. Mol. Catal. A: Chem.* **2005**, *241*, 79−87.

(21) Tashkova, K. A.; Andreev, A. *J. Mol. Struct.* **1984**, *115*, 55−58.

(22) Mukherjee, S.; Samanta, S.; Roy, B. C.; Bhaumik, A. *Appl. Catal., A* **2006**, *301*, 79–88.

(23) Singha, U. G.; Williams, R. T.; Hallamb, K. R.; Allen, G. C. *J. Solid State Chem.* **2005**, *178*, 3405–3413.

(24) Annis, D. A.; Jacobsen, E. N. *J. Am. Chem. Soc.* **1999**, *121,* 4147–4154.

(25) Clever, G. H.; Polborn K.; Carell, T. *Angew. Chem., Int. Ed.* **2005**, *44*, 7204−7208.

(26) Desai, M. N.; Desai, M. B.; Shah, C. B.; Desai, S. M. *Corros. Sci.* **1986**, *26*, 827−837.

(27) Gomma, G. K.; Wahdan, M. H. *Mater. Chem. Phys.* **1995**, *39*, 209−213.

(28) Li, S.; Chen, S.; Lei, S.; Ma, H.; Yu, R.; Liu, D. *Corros. Sci.* **1999**, *41*, 1273−1287.

(29) Ashassi-Sorkhabi, H.; Shabani, B.; Aligholipour, B.; Seifzadeh, D. *Appl. Surf. Sci.* **2006**, *252*, 4039−4047.

(30) Quan, Z.; Chen, S.; Li, Y.; Cui, X. *Corros. Sci.* **2002**, *44*, 703−715.

(31) Li, S. L.; Wang, Y. G.; Chen, S. H.; Yu, R.; Lei, S. B.; Ma, H. Y.; Liu, De X. *Corros. Sci.* **1999**, *41* 1769−1782.

(32) Quan, Z.; Chen, S.; Li, Y. *Corros. Sci.* **2001**, *43*, 1071−1080.

(33) Shokry, H.; Yuasa, M.; Sekine, I.; Issa, R. M.; El-Baradie, H. Y.; Gomma, G. K. *Corros. Sci.* **1998**, *39*, 1062–1075.

(34) Bilgiç, S.; Çaliskan, N. *J. Appl. Electrochem.* **2001**, *31*, 79–83.

(35) Hosseini, M.; Mertens, S. F. L.; Ghorbani, M.; Arshadi, M. R. *Mater. Chem. Phys.* **2003**, *78*, 800–808.

(36) Emregül, K. C.; Atakol, O. *Mater. Chem. Phys.* **2003**, *82*, 188–193.

(37) Emregül, K. C.; Kurtaran, R.; Atakol, O. *Corros. Sci.* **2003**, *45*, 2803–2817.

(38) Yurt, A.; Balaban, A.; Ustün Kandemir, S.; Bereket, G.; Erk, B. *Mater. Chem. Phys.* **2004**, *85*, 420–426.

(39) Ashassi-Sorkhabi, H.; Shaabani, B.; Seifzadeh, D. *Appl. Surf. Sci.* **2005**, *239*, 154–164.

(40) Ashassi-Sorkhabi, H.; Shaabani, B.; Seifzadeh, D. *Electrochim. Acta* **2005**, *50*, 3446–3452.

(41) Emregül, K. C.; Abdülkadir Akay, A.; Atakol, O. *Mater. Chem. Phys.* **2005**, *93*, 325–329.

(42) Yurt, A.; Bereket, G.; Kivrak, A.; Balaban, A.; Erk, B. *J. Appl. Electrochem.* **2005**, *35*, 1025–1032.

(43) Emregül, K. C.; Hayvalí, M. *Corros. Sci.* **2006**, *48*, 797–812.

(44) Mahajan, R. K.; Kaur, I.; Kumar, M. *Sens. Actuators, B* **2003**, *91*, 26–31.

(45) Abbaspour, A.; Esmaeilbeig, A.R.; Jarrahpour, A. A.; Khajeh, B.; Kia, R. *Talanta* **2002**, *58*, 397–403.

(46) Gupta, V. K.; Singh, A. K.; Mehtab, S.; Gupta, B. *Anal. Chim. Acta* **2006**, *566*, 5–10.

(47) Gupta, V. K.; Goyal, R. N.; Bachheti, N.; Singh, L. P.; Agarwal, S. *Talanta* **2005**, *68*, 193–197.

(48) Ganjali, M. R.; Golmohammadi, M.; Yousefi, M.; Norouzi, P.; Salavati-Niasari, M.; Javanbakht, M. *Anal. Sci.* **2003**, *19*, 223–227.

(49) Oshima, S.; Hirayama, N.; Kubono, K.; Kokusen, H.; Honjo, T. *Anal. Sci.* **2002**, *18*, 1351–1355.

(50) Alizadeh, N.; Ershad, S.; Naeimi, H.; Sharghi, H.; Shamsipur, M. *Fres. J. Anal. Chem.* **1999**, *365*, 511–515.

(51) Ganjali, M. R.; Poursaberi, T.; Babaei, L. H.; Rouhani, S.; Yousefi, M.; Kargar-Razi, M.; Moghimi, A.; Aghabozorg, H.; Shamsipur, M. *Anal. Chim. Acta* **2001**, *440*, 81–87.

(52) Ganjali, M. R.; Emami, M.; Rezapour, M.; Shamsipur, M.; Maddah, B.; Salavati-Niasari, M.; Hosseini, M.; Talebpoui, Z. *Anal. Chim. Acta* **2003**, *495*, 51–59.

(53) Mashhadizadeh, M. H.; Sheikhshoaie, I. *Talanta* **2003**, *60*, 73–80.

(54) Jain, A. K.; Gupta, V. K.; Ganeshpure, P. A.; Raisoni, J. R. *Anal. Chim. Acta* **2005**, *553*, 177–184.

(55) Jeong, T.; Lee, H. K.; Jeong, D. C.; Jeon, S. *Talanta* **2005**, *65*, 543–548.

(56) Ganjali, M.R.; Daftani, A.; Nourozi, P.; Salavati-Niasari, M. *Anal. Lett.* **2003**, *36*, 1511–1522.

(57) Gupta, V. K.; Agarwal, S.; Jakob, A.; Lang, H. *Sens. Actuators, B* **2006**, *114*, 812–818.

(58) Nielsen, M.; Larsen, N. B.; Gothelf, K. V. *Langmuir* **2002,** *18,* 2795−2799.

(59) Beulen, M. W. J.; van Veggel F. C. J. M.; Reinhoudt, D. N. *Isr. J. Chem.* **2000**, *40*, 73−80.

(60) Zell, P.; Mögele, F.; Ziener, U.; Rieger, B. *Chem.−Eur. J.* **2006**, *12*, 3847−3857.

(61) Zell, P.; Mögele, F.; Ziener, U.; Rieger, B. *J. Chem. Soc., Chem. Commun.* **2005**, 1294−1296.

(62) Qian, P.; Nanjo, H.; Sanada, N.; Yokoyama, T.; Suzuki, T. M. *Chem. Lett.* **2000**, 1118−1119.

(63) Sakata, I.; Miyamura, K. *J. Chem. Soc., Chem. Commun.* **2003**, 156−157.

(64) Whitesides, G. M. *Small* **2005**, *1*, 172–179.

(65) Moav, T.; Hatzor, A.; Cohen, H.; Libman, J.; Rubinstein, I.; Shanzer, A. *Chem.–Eur. J.* **1998**, *4*, 502−507.

(66) Gothelf, K. V.; Thomsen, A.; Nielsen, M.; Cló, E.; Brown, R. S. *J. Am. Chem. Soc.* **2004**, *126*, 1044−1046.

(67) Mendes, P. M.; Preece, J. A. *Curr. Opin. Colloid Interface Sci.* **2004**, *9*, 236– 248.

(68) Riu, J.; Maroto, A.; Rius F. X. *Talanta* **2006**, *69*, 288–301.

(69) Ozin, G. A.; Manners, I.; Fournier-Bidoz, S.; Arsenault, A. *Adv. Mater.* **2005**, *17*, 3011–3018.

(70) Balzani, V. *Small*, **2005**, *1*, 278–283.

(71) Aviram, A.; Ratner M. A. *Chem. Phys. Lett.* **1974**, *29*, 277–283.

(72) Shinkai, S.; Manabe, O. *Top. Curr. Chem.* **1984**, *121*, 67–104.

(73) Credi, A.; B. Ferrer Ribera, B.; Venturi, M. *Electrochim. Acta* **2004**, *49*, 3865–3872.

(74) Balzani, V.; Credi, A.; Raymo, F. M.; Stoddart, J. F. *Angew. Chem., Int. Ed.* **2000**, *39*, 3348–3391.

(75) Joachim, C.; Launay, J. P. *Nouv. J. Chim.* **1984**, *8*, 723–728.

(76) Lehn, J.-M. *Angew. Chem.* **1988**, *100*, 91–116.

(77) Shigekawa, H.; Takeuchi, O.; Aoyama, M. *Sci. Technol. Adv. Mater.* **2005**, *6*, 582–588.

(78) Palmer, R. E. *Surf. Interface Anal.* **2002**, *34*, 3–9.

(79) Rao, C. N. R.; Cheetham, A. K. *J. Mater. Chem.*, **2001**, *11*, 2887–2894.

(80) Ulman, A.; Kang, J. F.; Shnidman, Y.; Liao, S.; Jordan, R.; Choi, G.-Y.; Zaccaro, J.; Myerson, A. S.; Rafailovich, M.; Sokolov, J.; Fleischer, C. *Rev. Mol. Biotechnol.* **2000**, *74*, 175–188.

(81) Greig, L. M.; Philp, D. *Chem. Soc. Rev.* **2001**, *30*, 287–302.

(82) Layer, R. W. *Chem. Rev. (Washington, DC, U.K.)* **1963**, *63*, 489−510.

(83) Duffaut, N.; Dupin, J. P., *Bull. Soc. Chim. Fr.* **1966**, 3205−3210.

(84) Kafka, S.; Kappe, T., *Monatsh. Chem.* **1997**, *128*, 1019−1031.

(85) Eisch, J. J.; Sanchez, R. *J. Org. Chem.* **1986**, *51*, 1848–1852.

(86) Drew, E. W.; Ritchie, P. D. *Chem. Ind. (London)* **1952**, 1104.

(87) Reddelien, *G. Ber. Dt. Chem. Ges.* **1914**, *46*, 2712–2717.

(88) Walia, J. S.; Heindl, L.; Lader, H.; Walia, P. S. *Chem. Ind. (London)* **1968,** 155.

(89) Cho, B.R.; Oh, Y. C.; Lee, S. H.; Park, Y. J. *J. Org. Chem.* **1996**, *61*, 5656–5658.

(90) Fessenden, R. J.; Fessenden, J. S. *Organic Chemistry*, 6th edition, Brooks/Cole Publishing Company, USA, 1998, pp 563−564.

(91) Streitwieser, A.; Heathcock, C. H.; Kosower, E. M. *Introduction to Organic Chemistry*, 4th ed., Prentice Hall, New Yersey USA, 1998.

(92) Pärssinen, A.; Luhtanen, T.; Klinga, M.; Pakkanen, T.; Leskelä, M.; Repo, T. *Eur. J. Inorg. Chem.* **2005**, 2100–2109.

(93) Lai, Y.-C.; Chen, H.-Y.; Hung, W.-C.; Lin, C.-C.; Hong, F.-E. *Tetrahedron* **2005**, *61*, 9484–9489.

(94) Kettunen, M.; Abu-Surrah, A. S.; Abdel-Halim, H. M.; Repo, T.; Leskelä, M.; Laine, M.; Mutikainen, I.; Ahlgren, M. *Polyhedron* **2004**, *23*, 1649–1656.

(95) Weingarten, H. I.; White, W. A.; Chupp, J. P., *U.S. Pat. 3,636,110* **1972**.

(96) Weingarten, H.; Chupp, J. P.; White, W. A., *J. Org. Chem.* **1967**, *32*, 3246−3249.

(97) Blomberg, R. N.; Bruce, W. F., *U.S. Pat. 2,700,681* **1955**.

(98) Blomberg, R. N.; Bruce, W. F., *U.S. Pat. 2,700,682* **1955**.

(99) Forquy, C. *U.S. Pat. 5,406,000* **1995**.

(100) Disteldorf, J.; Huebel, W., Broschinski, L. *U.S. Pat. 4,429,157* **1984**.

(101) Hayashi, H.; Kainoh, A.; Katayama, M.; Kawasaki, K.; Okazaki, T., *Ind. Eng. Chem. Prod. Res. Dev.* **1976**, *15*, 299−303.

(102) see for example Filarowski, A.; Koll, A.; Kochel, A.; Kalenik, J.; Hansen, P.E. *J. Mol. Struct.* **2004**, *700*, 67–72.

(103) Binnemans, K.; Galyametdinov, Y. G.; van Deun, R.; Bruce, D. W.; Collinson, S. R.; Polishchuk, A. P.; Bikchantaev, I.; Haase, W.; Prosvirin, A. V.; Tinchurina, L.; Litvinov, I.; Gubajdullin, A.; Rakhmatullin, A.; Uytterhoeven, K.; van Meervelt, L. *J. Am. Chem. Soc.* **2000**, *122*, 4335−4344.

(104) Ready, J. M.; Jacobsen, E. N. *J. Am. Chem. Soc.* **2001**, *123*, 2687−2688.

(105) Haas, H. C.; Mass, A.; Moreau, R. D.; Nashua, N. H. *US4227013* **1980**.

(106) Haas H. C.; Moreau, R. D. *J. Polym. Sci. Polym. Chem. Ed.* **1978**, *16*, 699−700.

(107) Gilli, G., *Fundamentals of crystallography*, International Union of Crystallography: Oxford University Press, 1992, ed. Giacovacco, C., pp 468–473.

(108) Filarowski, A.; Koll, A.; Kochel, A.; Kalenik, J.; Hansen, P. E. *J. Mol. Struct.* **2004**, *700*, 67–72.

(109) Cimarelli, C.; Palmieri, G.; Volpini, E. *Tetrahedron* **2001**, *57*, 6089–6096.

(110) Cimarelli, C.; Palmieri, G. *Tetrahedron* **1998**, *54*, 15711–15720.
(111) Cimarelli, C.; Palmieri, G. *Tetrahedron* **2000**, *56*, 475–478.
(112) Neuvonen, K.; Pihlaja, K. J. *J. Chem. Soc., Perkin Trans. 2* **1988**, 461–467.
(113) Mason, A. F.; Coates, G. W. *J. Am. Chem. Soc.* **2004**, *126*, 16326–16327.
(114) Gerloch, M.; Lewis, J.; Mabbs, F. E.; Richards, A. *J. Chem. Soc. A* **1968**, 112–116.
(115) Abe, Y.; Nakabayashi, K.; Matsukawa, N.; Iida, M.; Tanase, T.; Sugibayashia; Ohta, K. *Inorg. Chem. Commun.* **2004**, *7*, 580–583.
(116) Paschke, R.; Balkow, D.; Sinn, E. *Inorg. Chem.* **2002**, *41*, 1949–1953.
(117) Miyamura, K.; Mihara, A.; Fujii, T.; Gohshi, Y.; Ishii, Y. *J. Am. Chem. Soc.* **1995**, *117*, 2377–2378.
(118) Paschke, R.; Balkow, D.; Baumeister, U.; Hartung, H.; Chipperfield, J. R.; Blake, A. B.; Nelson, P. G.; Gray, G. W. *Mol. Cryst. Liq. Cryst.* **1990**, *188*, 105–118.
(119) Blake, A. B.; Chipperfield, J. R. ; Hussain, W.; Paschke, R.; Sinn, E. *Inorg. Chem.* **1995**, *34,* 1125–1129.
(120) Hernandez-Molina, R.; Mederos, A.; Dominguez, S.; Gili, P.; Ruiz-Perez, C.; Castineiras, A.; Solans, X.; Lloret, F.; Real, J.A. *Inorg. Chem.* **1998**, *37*, 5102–5108.
(121) Zhang, Y.-L.; Ruan, W.-J.; Zhao, X.-J.; Wang, H.-G.; Zhu, Z.-A. *Polyhedron* **2003**, *22*, 1535–1545.
(122) Thomas, F.; Jarjayes, O.; Duboc, C.; Philouze, C.; Saint-Aman, E.; Pierre, J.-L. *J. Chem. Soc., Dalton Trans.* **2004**, 2662–2669.
(123) Elmali, A.; Elerman, Y.; Svoboda, I. *Acta Crystallogr., Sect. C: Cryst. Struct. Commun.* **2000**, *C56*, 423–424.
(124) Li, Z.-X.; Zhang, X.-L. *Acta Crystallogr., Sect. E: Struct. Rep. Online* **2004**, *E60*, m958–m959.
(125) Bunce, S.; Cross, R. J.; Farrugia, L. J.; Kunchandy, S.; Meason, L. L.; Muir, K. W.; O'Donnell, M. Peacock, R. D.; Stirling, D.; Teat, S. J. *Polyhedron* **1998**, *17*, 4179–4187.
(126) Gall, R. S.; Schaefer, W. P. *Inorg. Chem.* **1976**, *15*, 2758–2763.
(127) Calligaris, M.; Nardin, G.; Randaccio, L. *Coord. Chem. Rev.* **1972**, *7*, 385–403.
(128) Calligaris, M.; Minichelli, D.; Nardin, G.; Randaccio, L. *J. Chem. Soc. A* **1970**, 2411–2415.
(129) Hall, D.; Rae, A. D.; Waters, T. N. *J. Chem. Soc.* **1963**, 5897–5901.
(130) Hall, D.; Waters, T. N. *J. Chem. Soc.* **1960**, 2644–2648.
(131) Corazza, F.; Floriani, C.; Zehnder, M. *J. Chem. Soc., Dalton Trans.* **1987**, 709–714.

(132) Gerloch, M.; Mabbs, F. E. *J. Chem. Soc. A* **1967**, 1900–1908.

(133) Yamada, S. *Coord. Chem. Rev.* **1999**, *190-192*, 537–555.

(134) Sinn, E.; Harris, C. M. *Coord. Chem. Rev.* **1969**, *4*, 391–422.

(135) Fachinetti, G.; Floriani, C.; Zanazzi, P. F.; Zanzari, A. R. *Inorg. Chem.* **1979,** *18*, 3469–3475.

(136) Dreos, R.; Nardin, G.; Randaccio, L.; Siega, P.; Tauzher, G.; Vrdoljak, V. *Inorg. Chim. Acta* **2003**, *349*, 239–248.

(137) Schaefer, W. P.; Huie, B. T.; Kurilla, M. G.; Ealick, S. E. *Inorg. Chem.* **1980,** *19*, 340–344.

(138) Avdeef, A.; Schaefer, W. P. *J. Am. Chem. Soc.* **1976**, *98*, 5153–5159.

(139) Huie, B. T.; Leyden, R. M.; Schaefer, W. P. *Inorg. Chem.* **1979**, *18*, 125–129.

(140) Atkins, R.; Brewer, G.; Kokot, E.; Mockler, G. M.; Sinn, E. *Inorg. Chem.* **1985,** *24*, 127–134.

(141) Lashanizadegan, M.; Boghae, D. M. *Synth. React. Inorg., Met.-Org. Chem.* **2002**, *32*, 345–355.

(142) Bbadbhade, M. M.; Srinivas, D. *Inorg. Chem.* **1993**, *32*, 6122–6130.

(143) Glaser, T.; Heidemeier, M.; Grimme, S.; Bill, E. *Inorg. Chem.* **2004**, *43*, 5192–5194.

(144) Skovsgaard, S.; Bond, A. D.; McKenzie, C. J. *Acta Crystallogr., Sect. E: Struct. Rep. Online* **2005**, *E61*, m135–m137.

(145) Cheng, X.-L.; Gao, S.; Huo, L.-H.; Ng, S. W. *Acta Crystallogr., Sect E: Struct. Rep. Online* **2005**, *E61*, m385–m386.

(146) Averseng, F.; Lacroix, P. G.; Malfant, I.; Dahan, F.; Nakatani, K. *J. Mater. Chem.* **2000**, *10*, 1013–1018.

(147) Li, Z.; Jablonski, C. *Inorg. Chem.* **2000,** *39,* 2456–2461.

(148) *CRC Handbook of Chemistry and Physics*, Internet Version 2007 (87th ed.), ed. Lide, D. R., Taylor and Francis, Boca Raton, FL, 2007.

(149) Nakamoto, T.; Katada, M.; Endo, K.; Sano, H. *Polyhedron* **1998**, 17, 3507–3514.

(150) Li, G. Q.; Govind, R. *Ind. Eng. Chem. Res.* **1994**, *33*, 755−783.

(151) Szczepaniak, B.; Brągiel, P. *Vacuum* **1995**, *46*, 465−467.

(152) Tsumaki, T. *Bull. Chem. Soc. Jpn.* **1938**, *13*, 252−260.

(153) Bajdor, K.; Nakamoto, K.; Kanatomi, H.; Murase, I. *Inorg. Chim. Acta* **1984**, *82*, 207−210.

(154) Chen, D.; Martell, A. E. *Inorg. Chem.* **1987**, *26*, 1026−1030.

(155) Pui, A., *Croat. Chem. Acta* **2002**, *CCACAA 75*, 165−173.

(156) Bailes, R. H.; Calvin, M. *J. Am. Chem. Soc.* **1947**, *69*, 1886−1893.

(157) Cesarotti, E.; Gullotti, M.; Pasini, A.; Ugo, R. *J. Chem. Soc., Dalton Trans.* **1977**, 757−763.

(158) Floriani, C.; Calderazzo, F. *J. Chem. Soc. A* **1969**, 946–953.

(159) Calligaris, M.; Nardin, G.; Randaccio, L. *J. Chem. Soc., Dalton Trans.* **1973**, 419−424.

(160) Niederhoffer, E. C. ; Timmons, J. H.; Martell, A. E. *Chem. Rev. (Washington, DC, U.S.)* **1984,** 84, 137−203.

(161) Ortiz, B.; Park, S.-M. *Bull. Korean Chem. Soc.* **2000**, *21*, 405−411.

(162) Suzuki, M.; Ishiguro, T.; Kozuka, M.; Nakamoto, K. *Inorg. Chem.* **1981**, *20*, 1993−1996.

(163) Abel, E. W.; Pratt, J. M.; Whelan, R. *Inorg. Nucl. Chem. Lett.* **1971**, *7*, 901−904.

(164) Calligaris, M.; Nardin, G.; Randaccio, L.; Ripamonti, A. *J. Chem. Soc. A* **1970**, 1069–74.

(165) Kruger, P. E.; Moubaraki, B.; Murray, K. S.; Tiekink, E. R. T. *J. Chem. Soc., Dalton Trans.* **1994**, 2129–2134.

(166) Fenton, D. E.; Okawa, H. *J. Chem. Soc., Dalton Trans.* **1993**, 1349–1357.

(167) Bond, A. M.; Haga, M.; Creece, I. S.; Robson, R.; Wilson, J. C. *Inorg. Chem.* **1989**, *28*, 559–566.

(168) Farrugia, L. G.; Lovatt, P. A.; Peacock, R. D. *J. Chem. Soc., Dalton Trans.* **1997**, 911–912.

(169) Alexander, V. *Chem. Rev. (Washington, DC, U.S.)* **1995**, *95*, 273–342.

(170) Que, L.; True, A. E., Jr. *Prog. Inorg. Chem.* 1990, *38*, 97−200.

(171) Asokan, A.; Varghese, B.; Manoharan, P. T. *Inorg. Chem.* **1999**, *38*, 4393−4399.

(172) Furutachi, H.; Okawa, H. *Inorg. Chem.* **1997**, *36*, 3911−3918.

(173) Casellato, U.; Tamburini, S.; Tomasin, P.; Vigato, P. A. *Inorg. Chim. Acta* **2004**, *357*, 4191−4207.

(174) Schindler, S. *Eur. J. Inorg. Chem.* **2000**, 2311−2326.

(175) Guo, N.; Li, L.; Marks, T. J. *J. Am. Chem. Soc.* **2004**, *126*, 6542−6543.

(176) Esteruelas, M. A.; Garcia, M. P.; López, A. M.; Oro, L. A. *Organometallics* **1991**, *10*, (1991) 127−133.

(177) Molenveld, P.; Engbersen, J. F. J.; Reinhoudt, D. N. *Chem. Soc. Rev.* **2000**, *29*, 75−86.

(178) van den Beuken, E. K.; Feringa, B. L. *Tetrahedron* **1998**, *54*, 12985−13011.

(179) Brudenell, S. J.; Spiccia, L.; Bond, A. M.; Fallon, G. D.; Hockless, D. C. R.; Lazarev, G.; Mahon, P. J.; Tiekink, E. R. T. *Inorg. Chem.* **2000**, *39*, 881−892.

(180) Hascall, T.; Beck, V.; Barlow, S.; Cowley, A. R.; O'Hare, D. *Organometallics* **2004**, *23*, 3808−3813.

(181) Alvarez, S.; Palacios, A. A.; Aullo´n, G. *Coord. Chem. Rev.* **1999**, *185–186*, 431−450.

(182) Nakamura, M.; Okawa, H.; Kida, S. *Inorg. Chim. Acta* **1983**, *75*, 9–13.

(183) Kahn, O. *Adv. Inorg. Chem.* **1995**, *43*, 179−259.

(184) Tandon, S. S.; Thompson, L. K.; Brideson, J. N. *J. Chem. Soc., Chem. Commun.* **1993**, 804−806.

(185) Vigato, P. A.; Tamburini, S.; Fenton, D. E. *Coord. Chem. Rev.* **1990**, *106*, 25−170.

(186) Menif, R.; Martell, A. E.; Squattrito, P. J.; Clearfield, A. *Inorg. Chem.* **1990**, *29*, 4723−4729.

(187) *Surface Analysis Methods in Materials Science*, ed. O'Connor, D. J.; Sexton, B. A.; Smart, R. St. C., Springer-Verlag, Berlin Heidelberg 1992, pp 13, 35–38, 183, 221–244.

(188) *Encyclopedia of Materials Characterization, Surfaces, Interfaces, Thin Films*, ed. *Brundle, C. R.; Evans, C. A., Jr.; Wilson, S.; Fitzpatrick, L. E.* Butterworth-Heinemann, Boston 1992, pp 4, 9, 22, 85–98.

(189) van de Walle, G. F. A.; van Loenen, E. J.; Elswijk, H. B.; Hoeven, A. J., *Analysis of Microelectronic Materials and Devices*, ed. Grasserbauer, M.; Werner, H. W., John Wiley & Sons Ltd., England, 1996, pp 657−678.

(190) Holý, V.; Pietsch, U.; Baumbach, T. *High-Resolution X-Ray Scattering from Thin Films and Multilayers*, Springer-Verlag, Berlin Heidelberg 1999, pp 3-21, 128-134, 191-219.

(191) Binnig, G.; Quate, C. F.; Gerber, C. *Phys. Rev. Lett.* **1986**, *56*, 930–933.

(192) Samorí, P.; Rabe, J. P. *J. Phys.: Condens. Matter* **2002**, *14*, 9955–9973.

(193) Loos, J. *Adv. Mater.* **2005**, *17*, 1821-1833.

(194) Binnig, G.; Rohrer, H.; Gerber, C.; Weibel, E. *Appl. Phys. Lett.* **1982**, *40*, 178–180.

(195) Kleineberg, U.; Brechling, A.; Sundermann, M.; Heinzmann, U. *Adv. Funct. Mater.* **2001**, *11*, 208−212.

(196) Hla, S.-W. *J. Vac. Sci. Technol., B: Microelectron. Nanometer Struct.–Process., Meas., Phenom.* **2005**, *23*, 1351–1360.

(197) Hla, S.-W.; Rieder, K.-H. *Superlattices Microstruct.*, **2002**, *31*, 63–72.

(198) Lorente, N.; Rurali, R.; Tang, H. *J. Phys.: Condens. Matter.* **2005**, *17*, S1049–S1074.

(199) Gauthier, S. *Appl. Surf. Sci.* **2000**, *164*, 84–90.

(200) Prime, K. L.; Whitesides, G. M. *Science* (Washington, DC, U.S.) **1991**, *252*, 1164−1167.

(201) Bigelow, W. C.; Pickett, D. L.; Zisman, W. A. *J. Colloid Sci.* **1946**, *1*, 513−538.

(202) Nakamura, T.; Koyama, E.; Shimoi, Y.; Abe, S.; Ishida, T.; Tsukagoshi, K.; Mizutani, W.; Tokuhisa, H.; Kanesato, M.; Nakai, I.; Kondoh, H.; Ohta, T. *J. Phys. Chem. B* **2006,** *110,* 9195−9203.

(203) Ulman, A.; Evans, S. D.; Shnidman, Y.; Sharma, R.; Eilers, J. E.; Chang, J. C. *J. Am. Chem. Soc.* **1991**, *113*, 1499–1506.

(204) Herdt, G. C.; Jung, D. R.; Czanderna, A. W. *Prog. Surf. Sci.* **1995**, *50*, 103–129.

(205) Nogueira Diógenes, I. C.; Rodrigues de Sousa, J.; Moreira de Carvalho, I. M.; Arruda Temperini, M. L.; Tanaka, A. A.; de Sousa Moreira, Í. *J. Chem. Soc., Dalton Trans.* **2003**, 2231−2236.

(206) Nogueira Diógenes, I. C.; Nart, F. C.; Arruda Temperini, M. L.; de Sousa Moreira, Í. *Inorg. Chem.* **2001**, *40,* 4884−4889.

(207) Ulman, A. *Chem. Rev.* **1996**, *96*, 1533–1554.

(208) Schreiber, F. *Prog. Surf. Sci.* **2000**, *65*, 151–256.

(209) Tao, N. J. *Phys. Re*v. *Lett.* **1996**, *76*, 4066–4069.

(210) De Feyter, S.; De Schryver, F. C. *Chem. Soc. Rev.* **2003**, *32*, 139−150.

(211) Qiu, X.; Wang, C.; Zeng, Q.; Xu, B.; Yin, S.; Wang, H.; Xu, S.; Bai, C. *J. Am. Chem. Soc.* **2000**, *122,* 5550−5556.

(212) Shaporenko, A.; Brunnbauer, M.; Terfort, A.; Grunze, M.; Zharnikov, M *J. Phys. Chem. B* **2004**, *108*, 14462−14469.

(213) Flink, S.; van Veggel, F. C. J. M.; Reinhoudt, D. N. *Adv. Mater.* **2000**, *12*, 1315−1328.

(214) Su, C.; Shu, C.-R.; Wu, C.-C. *Liq. Cryst.* **2002**, *29*, 1169−1176.

(215) Smith, R. K.; Lewis, P. A.; Weiss, P. S. *Prog. Surf. Sci.* **2004**, *75*, 1–68.

(216) Sandhyarani, N.; Pradeep, T. *Int. Rev. Phys. Chem*. **2003**, *22*, 221–262.

(217) Lei, S. B.; Wang, C.; Yin, S. X.; Bai, C. L. *J. Phys. Chem. B.* **2001**, *105*, 12272−12277.

(218) Jin, Q.; Rodriguez, J. A.; Li, C. Z.; Darici, Y.; Tao, N. J. *Surf. Sci.* **1999**, *425*, 101–111.

(219) Mourran, A.; Ziener, U.; Möller, M.; Breuning, E.; Ohkita, M.; Lehn, J.-M. *Eur. J. Inorg. Chem.* **2005**, 2641−2647.

(220) Alam, M. S.; Strömsdörfer, S.; Dremov, V.; Müller, P.; Kortus, J.; Ruben, M.; Lehn, J.-M. *Angew. Chem., Int. Ed.* **2005**, *44*, 7896−7900.

(221) Yang, Z.-Y.; Gan, L.-H.; Lei, S.-B.; Wan, L.-J.; Wang, C.; Jiang, J.-Z. *J. Phys. Chem. B* **2005**, *109*, 19859−19865.

(222) Lu, X.; Li, M.; Yang, C.; Zhang, L.; Li, Y.; Jiang, L.; Li, H.; Jiang, L.; Liu, C.; Hu, W. *Langmuir* **2006**, *22*, 3035−3039.

(223) Zhang, Z.; Yoshida, N.; Imae, T.; Xue, Q.; Bai, M.; Jiang, J.; Liu, Z. *J. Colloid Interface Sci.* **2001**, *243***,** 382–387.

(224) Zhang, Z.; Imae, T. *Nano Lett.* **2001**, *1*, 241−243.

(225) Aswal, D.K.; Lenfant, S.; Guerin, D.; Yakhmi, J.V.; Vuillaume, D.; *Anal. Chim. Acta* **2006**, *568*, 84–108.

(226) Rittner, M.; Martin-Gonzalez, M. S.; Flores, A.; Schweizer, H.; Effenberger, F.; Pilkuhn, M. H. *J. Appl. Phys.* **2005**, *98*, 054312.

(227) Cotton, F. A.; Wilkinson, G.; Murillo, C. A.; Bochmann, M. *Advanced Inorganic Chemistry*, 5th edition, John Wiley & Sons Inc., New York 1988, pp 756, 757 and 939.

(228) Pearson, R. G.; Songstad, J. *J. Am. Chem. Soc.* **1967**, *89*, 1827−1836.

(229) Pearson, R. G. *J. Am. Chem. Soc.* **1963**, *85*, 3533−3539.

(230) Grönbeck, H.; Curioni, A.; Andreoni, W. *J. Am. Chem. Soc.* **2000**, *122*, 3839−3842.

(231) Taniguchi, I.; Iseki, M.; Yamaguchi, H.; Yasukouchi, K. *J. Electroanal. Chem.* **1985**, *186*, 299−307.

(232) Whitesides, G. M.; Laibinis, P.E. *Langmuir* **1990**, *6*, 87−96.

(233) Sawaguchi, T.; Mizutani, F.; Taniguchi, I. *Langmuir* **1998**, *14*, 3565−3569.

(234) Lamp, B. D.; Hobara, D.; Porter, M. D.; Niki, K.; Cotton, T. M. *Langmuir* **1997**, *13*, 736−741.

(235) Cavalleri, O.; Prato, M.; Chincarini, A.; Rolandi, R.; Canepa, M.; Gliozzi, A.; Alloisio, M.; Lavagnino, L.; Cuniberti, C.; Dell'Erba, C.; Dellepiane, G. *Appl. Surf. Sci.* **2005**, *246*, 403−408.

(236) Sondag-Huethorst, J. A. M.; Schönenberger, C.; Fokkink, L. G. J. *J. Phys. Chem.* **1994**, *98*, 6826−6834.

(237) Rong, H.-T.; Frey, S.; Yang, Y.-J., Zharnikov, M.; Buck, M.; Wühn, M.; Wöll, C.; Helmchen, G. *Langmuir* **2001**, *17*, 1582−1593.

(238) Bucher, J.-P.; Santesson, L.; Kern, K. *Langmuir* **1994**, *10*, 979−983.

(239) Fuxen, C.; Azzam, W.; Arnold, R.; Witte, G.; Terfort, A.; Wöll, C. *Langmuir* **2001**, *17*, 3689−3695.

(240) Cavalleri, O.; Hirstein, A.; Kern, K. *Surf. Sci.* **1995**, *340*, L960−L964.

(241) Azzam, W.; Cyganik, P.; Witte, G.; Buck, M.; Wöll, Ch. *Langmuir* **2003**, *19*, 8262−8270.

(242) Cyganik, P.; Buck, M.; Azzam, W.; Wöll, Ch. *J. Phys. Chem. B* **2004**, *108*, 4989−4996.

(243) Delamarche, E.; Michel, B.; Kang, H.; Gerber, Ch. *Langmuir* **1994**, *10*, 4103−4108.

(244) McCarley, R. L.; Dunaway, O. J.; Willicut, R. J. *Langmuir* **1993**, *9*, 2775−2777.

(245) Mortier, T.; Persoons, A.; Verbiest, T. *Inorg. Chem. Comm.* 2005, *8*, 1075−1077.

(246) Arakawa, E. T.; Chung, M. S.; Williams, M. W. *Rev. Sci. Instrum.* **1977**, *48*, 707−708.

(247) Kalousek, J., Malát, V. *Czech. J. Phys. B* **1967**, *17*, 480−481.

(248) Valenzuela, A., Eckardt, J. C. *Rev. Sci. Instrum.* **1971**, *42*, 127−128.

(249) Lovell, S.; Rollinson, E. *J. Sci. Instrum.* **1968**, *1*, 1032–1035.

(250) Pashley, D. W. *Adv. Phys.* **1956**, *5*, 173–240.

(251) Ding, Y.; Kim, Y.-J.; Erlebacher, J. *Adv. Mater.* **2004**, *16*, 1897–1900.

(252) Greenwood, N. N.; Earnshaw, A.; *Chemistry of the Elements*, 2nd edition, Butterworth-Heinemann: Oxford, 1997, pp 274−275.

(253) SPI Supplies Catalogue http://www.2spi.com/catalog/new/hopgsub.shtml

(254) Ladd, J.; Boozer, C.; Yu, Q.; Chen, S.; Homola, J.; Jiang, S. *Langmuir* **2004**, *20*, 8090–8095.

(255) Huan, S; Shen, G.; Yu, R. *Electroanalysis* **2004**, *16*, 1019–1023.

(256) Maya, F.; Flatt, A. K.; Stewart, M. P.; Shen, D. E.; Tour, J. M. *Chem. Mater.* **2004**, *16*, 2987–2997.

(257) Flink, S.; Boukamp, B. A.; van den Berg, A.; van Veggel, F. C. J. M.; Reinhoudt, D. N. *J. Am. Chem. Soc.* **1998**, *120*, 4652–4657.

(258) Sehlotho, N.; Nyokong, T. *Electrochim. Acta* **2006**, *51*, 4463–4470.

(259) Lu, X.; Lv, B.; Xue, Z.; Li, M.; Zhang, L.; Kang, J. *Thin Solid Films* **2005**, *488*, 230−235.

(260) Zhang, Q.; Archer, L. A. *J. Phys. Chem. B* **2003,** *107,* 13123−13132.

(261) Zhou, Y.; Jiang, S.; Ğağın, T.; Yamaguchi, E. S.; Frazier, R.; Ho, A.; Tang, Y.; Goddard, W. A. III *J. Phys. Chem. B* **2000,** *104*, 2508−2524.

(262) Quon, R. A.; Ulman, A.; Vanderlick, T. K. *Langmuir* **2000**, *16*, 3797–3802.

(263) Gupta, P.; Loos, K.; Korniakov, A.; Spagnoli, C.; Cowman, M.; Ulman, A. *Angew. Chem., Int. Ed.*, **2004**, *43*, 520–523.

(264) Srivastava, P.; Chapman, W. G.; Laibinis, P. E. *Langmuir*, **2005**, *21*, 12171–12178.

(265) Aray, Y.; Rodríguez, J.; Santiago Coll, D.; Gonzalez, C.; Marquez, M. *J. Phys. Chem. B*, **2004**, *108*, 18942–18948.

(266) Zhang, L.; Dong, B.; Huo, F.; Zhang, X.; Chi, L.; Jiang, L. *J. Chem. Soc., Chem. Commun.* **2001**, *19*, 1906–1907.

(267) Bettelheim, A.; Soifer, L.; Korin, E. *J. Electroanal. Chem.* **2004**, *571*, 265–272.

(268) Eberspacher, T. A.; Collman, J. P.; Chidsey, C. E. D.; Donohue, D. L.; Van Ryswyk, H. *Langmuir* **2003,** *19,* 3814−3821.

(269) Ciszek, J. W.; Keane, Z. K.; Cheng, L.; Stewart, M. P;Yu, L. H.; Natelson, D.; Tour, J. M.; *J. Am. Chem. Soc.* **2006**, *128*, 3179−3189.

(270) Mashazi, P. N.; Ozoemena, K. I.; Maree, D. M.; Nyokong, T. *Electrochim. Acta* **2006**, *51*, 3489–3494.

(271) Ozoemena, K. I.; Nyokong, T. *Microchem. J.* **2003**, *75*, 241−247.

(272) Stolarczyk, K.; Bilewicz, R.; Siegfried, L.; Kaden, T. *Inorg. Chim. Acta* **2003**, *348*, 129−134.

(273) Soto, E.; MacDonald, J. C.; Cooper, C. G. F.; McGimpsey, W. G. *J. Am. Chem. Soc.* **2003**, *125*, 2838−2839.

(274) Ehler, T. T.; Malmberg, N.; Carron, K.; Sullivan, B. P.; Noe, L. J. *J. Phys. Chem. B* **1997**, *101,* 3174−3180.

(275) Lacroix, P. G. *Eur. J. Inorg. Chem.* **2001**, 339−348.

(276) Rivera, J. M.; Guzmán, D.; Rodriguez, M.; Lamère, J. F.; Nakatani, K.; Santillan, R.; Lacroix, P. G.; Farfán, N. *J. Organomet. Chem.* **2006**, *691*, 1722–1732.

(277) Di Bella, S. *Chem. Soc. Rev.* **2001**, *30*, 355-366.

(278) Dunn, J. D.; Watson, J. T.; Bruening, M. L. *Anal. Chem.* **2006**, *78*, 1574−1580.

(279) Kalyuzhny, G.; Vaskevich,A.; Ashkenasy, G.; Shanzer, A.; Rubinstein, I. *J. Phys. Chem. B* **2000**, *104,* 8238−8244.

(280) Sawaguchi, T.; Mizutani, F.; Yoshimoto, S.; Taniguchi, I. *Electrochim. Acta* **2000**, *45*, 2861–2867.

(281) Snopok, B. A.; Boltovets, P. N.; Tsymbal, L. V.; Lampeka, Ya. D., *Theor. Exp. Chem.* **2004**, *40*, 260−265.

(282) Tian, Z. Q. *J. Raman Spectrosc.* **2005**, *36*, 466–470.

(283) Tao, F.; Cai, Y.; Bernasek, S. L. *Langmuir* **2005**, *21*, 1269–1276.

(284) Su, C.; Yu, S.-H.; Shu, C.-R.; Wang, H.-H.; Lai, C.-K. *Synth. Met.* **2003**, *137*, 915–916.

(285) Spong, J. K.; Mizes, H. A.; LaComb, L. J., Jr.; Dovek, M.M.; Frommer, J. E.; Foster, J. S. *Nature* (London, U.K.) **1989**, *338*, 137−138.

(286) Foster, J. S.; Frommer, J. E. *Nature (London, U.K.)* **1988**, *333*, 542−545.

(287) Cyr, D. M.; Venkataraman, B.; Flynn, G. W. *Chem. Mater.* **1996**, *8*, 1600−1615.

(288) Lei, S. B.; Wang, C.; Wan, L. J.; Bai, C. L. *J. Phys. Chem. B.* **2004**, *108*, 1173−1175.

(289) Xu, B.; Yin, S. X.; Wang, C.; Qiu, X. H.; Zeng, Q. D.; Bai, C. L. *J. Phys. Chem. B.* **2000**, *104*, 10502−10505.

(290) Lei, S. B.; Yin, S. X.; Wang, C.; Wan, L. J.; Bai, C. L. *Chem. Mater.* **2002**, *14*, 2837−2838.

(291) Ohshiro, T.; Ito, T.; Buhlmann, P.; Umezawa, Y. *Anal. Chem.* **2001**, *73*, 878−883.

(292) Ikeda, T.; Asakawa, M.; Goto, M.; Miyake, K.; Ishida, T.; Shimizu, T. *Langmuir* **2004,** *20,* 5454−5459.

(293) Ogunrinde, A.; Hipps, K. W.; Scudiero, L. *Langmuir* **2006**, *22*, 5697–5701.

(294) Wang, Z.; Zeng, Q.; Wan, L.; Wang, C.; Yin, S.; Bai, C.; Wu, X.; Yang, J. *Surf. Sci.* **2002**, *513*, L436−L440.

(295) Wedeking, K.; Mu, Z.; Kehr, G.; Fröhlich, R.; Erker, G.; Chi, L.; Fuchs, H. *Langmuir* **2006**, *22*, 3161−3165.

(296) Wedeking, K.; Mu, Z.; Kehr, G.; Cano Sierra, J.; Mück, Lichtenfeld, C.; Grimme, S.; Erker, G.; Fröhlich, R.; Chi, L.; Wang, W.; Zhong, D.; Fuchs, H. *Chem.−Eur. J.* **2006**, *12*, 1618−1628.

(297) Semenov, A.; Spatz, J. P.; Möller, M.; Lehn, J.-M.; Sell, B.; Schubert, D.; Weidl, C. H.; Schubert, U. S. *Angew. Chem., Int. Ed.* **1999**, *38*, 2547−2550.

(298) De Feyter, S.; Abdel-Mottaleb, M. M. S.; Schuurmans, N.; Verkuijl, B. J. V.; van Esch, J. H.; Feringa, B. L.; De Schryver, F. C. *Chem.−Eur. J.* **2004**, *10*, 1124−1132.

(299) Hobday, M. D.; Smith, T. D. *Coord. Chem. Rev.* **1972-1973**, *9*, 311−337.

(300) Desiraju, G. R. *J. Chem. Soc., Chem. Commun.* **2005**, 2995–3001.

(301) Räisänen, M. T.; Mögele, F.; Feodorow, S.; Rieger, B.; Ziener, U.; Leskelä, M.; Repo, T. unpublished results.

(302) Claypool, C. L.; Faglioni, F.; Goddard, W. A. , III; Gray, H. B.; Lewis, N. S.; Marcus, R. A. *J. Phys. Chem. B* **1997**, *101*, 5978–5995.

(303) Constable E. C.; Häusler, M.; Hermann, B. A.; Housecroft, C. E.; Neuburger, M.; Schaffner, S.; Scherer, L. J. *Cryst. Eng. Commun.* **2007**, *9*, 176–180.

(304) Kim, K.; Matzger, A. J. *J. Am. Chem. Soc.* **2002**, *124*, 8772–8773.

(305) Constable E. C.; Güntherodt, H.-J.; Housecroft, C. E.; Merz, L.; Neuburger, M.; Schaffner, S.; Tao, Y. *New. J. Chem.* **2006**, *30*, 1470–1479.

(306) De Feyter, S.; Gesquière, A.; Wurst, K.; Amabilino, D. B.; Veciana, J.; De Schryver, F. C. *Angew. Chem., Int. Ed.* **2001**, *40*, 3217–3220.

(307) Azumi, R.; Götz, G.; Debaerdemaeker, T.; Bäuerle, P. *Chem.−Eur. J.* **2000**, *6*, 735–744.

(308) Eichhorst-Gerner, K.; Stabel, A.; Moessner, G.; Declerq, D.; Valiyaveettil, S.; Enkelmann, V.; Müller, K.; Rabe, J. P. *Angew. Chem., Int. Ed.* **1996**, *35*, 1492–1495.

(309) Lei, S. B.; Wang, C.; Yin, S. X.; Wang, H. N.; Xi, F.; Liu, H. W.; Xu, B.; Wan, L. J.; Bai, C. L. *J. Phys. Chem. B* **2001**, *105*, 10838–10841.

(310) Azumi, R.; Mena-Osteritz, E.; Boese, R.; Benet-Buchholz, J.; Bäuerle, P. *J. Mater. Chem.* **2006**, *16*, 728–735.